J|A|C|S
ARTICLES
Published on Web 05/31/2002

Reactivity of Phosphate Monoester Monoanions in Aqueous Solution. 1. Quantum Mechanical Calculations Support the Existence of "Anionic Zwitterion" $MeO^+(H)PO_3^{2-}$ as a Key Intermediate in the Dissociative Hydrolysis of the Methyl Phosphate Anion[1]

Marc Bianciotto,[†] Jean-Claude Barthelat,[‡] and Alain Vigroux*,[†]

Contribution from the Laboratoire de Synthèse et Physico-Chimie de Molécules d'Intérêt Biologique (UMR 5068), and Laboratoire de Physique Quantique, IRSAMC (UMR 5626), Université Paul Sabatier, 118 Route de Narbonne, 31062 Toulouse Cedex 4, France

Received January 18, 2002

Abstract: The dissociative hydrolysis reaction of the methyl phosphate monoanion has been studied for the reactant species $CH_3OPO_3H^-$ (**1**) and $CH_3OPO_3H^-\cdot H_2O$ (**1a**) in the gas and aqueous phases by density functional theory (B3LYP) calculations. Nonspecific solvation effects were taken into account with the polarizable continuum model PCM either by solvating the gas-phase reaction paths or by performing geometry searches directly in the presence of the solvation correction. In agreement with previous theoretical studies, our gas-phase calculations indicate that proton transfer to the methoxy group of **1** is concerted with P−O bond cleavage. In contrast, optimizations performed with the PCM solvation model establish the existence of the tautomeric form $CH_3O^+(H)PO_3^{2-}$ (**2**) as an intermediate, indicating that proton transfer and P−O bond cleavage become uncoupled in aqueous solution. The dissociative pathway of **1a** is energetically favored over the dissociative pathway of **1** only when the added water molecule plays an active catalytic role in the prototropic rearrangement **1** ↔ **2**. In that case, it is found that the collapse (via P−O bond cleavage) of the hydrated zwitterionic form $CH_3O^+(H)PO_3^{2-}\cdot H_2O$ (**2a**) is rate-determining. This collapse may occur by a stepwise mechanism through a very short-lived metaphosphate intermediate (PO_3^-), or by a concerted S_N2-like displacement through a loose metaphosphate-like transition state. The present calculations do not allow a distinction to be made between these two alternatives, which are both in excellent agreement with experiment. The present study also reveals that PO_3^- reacts selectively with CH_3OH and H_2O nucleophiles in aqueous solution. However, the observed selectivity of metaphosphate is governed by solvation effects, not nucleophilicity (water being much more effective than methanol in capturing PO_3^-). This arises from a better solvation of the addition product $H_2O^+PO_3^{2-}$ as compared to $CH_3O^+(H)PO_3^{2-}$.

Introduction

The enzyme-catalyzed cleavage of phosphate ester bonds is an essential and ubiquitous reaction in biological systems.[2] Crucial to an understanding of the mode of action of enzymes that catalyze phosphoryl ($-PO_3^{2-}-$) transfer, including kinases, phosphatases, and Ras and other G proteins, is knowledge of the mechanisms of the simple nonenzymatic hydrolysis reactions. Reactions of unprotonated and singly protonated phosphate monoesters resulting in hydrolysis or transfer of the phosphoryl group can, in principle, occur by two limiting mechanisms: those called *dissociative*, which proceed via the hydrated metaphosphate ion PO_3^- (eq 1), and those called *associative*, which require the formation of an intermediate or transition state with pentacovalent phosphorus (eq 2).

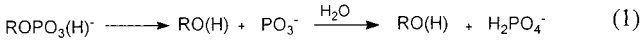

(1)

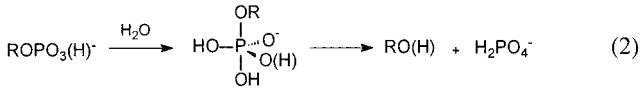

(2)

Although the enzyme-catalyzed reactions of phosphate monoesters are often interpreted in terms of whether the reaction pathway is associative or dissociative,[3] it is generally believed that the corresponding reactions in solution are dissociative.[4] However, this "dogma" has been challenged by recent theoreti-

* To whom correspondence should be addressed. E-mail: vigroux@chimie.ups-tlse.fr. Fax: (+33) 5-61-55-60-11.
[†] Laboratoire de Synthèse et Physico-Chimie de Molécules d'Intérêt Biologique.
[‡] Laboratoire de Physique Quantique.

(1) Part 2: Bianciotto, M.; Barthelat, J.-C.; Vigroux, A. *J. Phys. Chem. A*, in press.
(2) Westheimer, F. H. *Science* **1987**, *235*, 1173.
(3) For reviews, see: (a) Knowles, J. R. *Annu. Rev. Biochem.* **1980**, *49*, 877. (b) Gerlt, J. A. In *The Enzymes*, 3rd ed.; Sigman, D. S., Ed.; Academic Press: New York, 1992; Vol. 20, pp 95−139. (c) Maegley, K. A.; Admiraal, S. J.; Herschlag, D. *Proc. Natl. Acad. Sci. U.S.A.* **1996**, *93*, 8160. (d) Admiraal, S. J.; Herschlag, D. *Chem. Biol.* **1995**, *2*, 729. (e) Gani, D.; Wilkie, J. *Chem. Soc. Rev.* **1995**, 55.

cal studies,[5,6] in which it has been demonstrated that the arguments brought traditionally to support the dissociative mechanism could be interpreted equally well as evidence for the associative mechanism.

The monoester monoanion reaction is usually considered much less relevant to the understanding of enzyme catalysis than the monoester dianion reaction. However, recent modeling studies[7,8] on protein kinase and protein phosphatase enzymes support that, for these systems in which there is a conserved aspartate residue (Asp) in close proximity to a phosphate group in the active site, protonation of the phosphate (to a monoanion) rather than Asp is favored. Thus, possible enzyme mechanisms involving the (singly protonated) monoanion should also be considered in a careful analysis.

For monoesters of alcohols and phenols of $pK_a > 5.5$, it is well known that the monoanions, whose concentration peaks at pH $\approx$ 4, hydrolyze by P−O bond cleavage much faster than the corresponding dianionic species.[9] This observation has been attributed to intramolecular protonation of the leaving group oxygen. This provides both an internal nucleophile in the form of two oxyanions and an activated alcohol leaving group. Proton transfer may occur either in a rapid pre-equilibrium step, or simultaneously with leaving group departure, depending upon the basicity of the leaving group, as shown in Scheme 1.[10] Nor can one exclude the possibility of the involvement of a solvent water molecule in the proton transfer. The six-membered ring formed in the reaction with participation of water may be less strained than the four-membered ring without water.

However, as mentioned above, the groups of Åqvist and Warshel have recently shown that most of the experimental data about phosphate monoester hydrolysis does not provide the required information for deciding whether the mechanism is dissociative or associative.[5] On the basis of earlier theoretical studies,[6,13] it was argued that the often cited evidence for the dissociative mechanism is, in fact, equally consistent with an alternative associative mechanism, substrate-assisted general base catalysis, in which a pre-equilibrium proton transfer takes place from water to either the monoanion (eq 3) or the dianion (eq 4), followed by hydroxide ion attack on the resulting neutral (eq 3) or monoanionic (eq 4) phosphate monoester.

Scheme 1. Pathway for Dissociative Hydrolysis (by P−O Bond Cleavage) of Phosphate Monoester Monoanions[a]

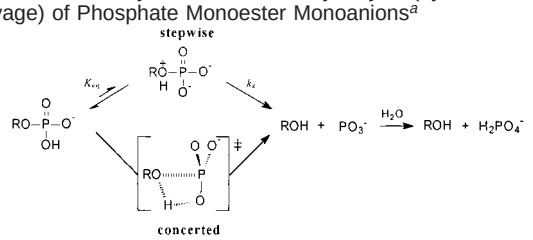

[a] Proton transfer to the leaving group may occur in a pre-equilibrium step (top), or simultaneously with leaving group departure (bottom), depending upon the basicity of the leaving group; see footnote 10.

$$H_2O + ROPO_3H^- \overset{K_{eq}}{\rightleftharpoons} OH^- + ROPO_3H_2 \xrightarrow{k} ROH + H_2PO_4^- \quad (3)$$

$$H_2O + ROPO_3^{2-} \overset{K_{eq}}{\rightleftharpoons} OH^- + ROPO_3H^- \xrightarrow{k} ROH + HPO_4^{2-} \quad (4)$$

Thus, despite considerable kinetic data accumulated over the past 45 years, the mechanism for the hydrolysis of methyl phosphate, the simplest phosphate ester, still has to be cleared up. In the absence of unequivocal experimental facts, electronic structure calculations become a valuable alternative. In a theoretical study,[14] Florian and Warshel have investigated the energetics of the associative and dissociative mechanisms for the methyl phosphate ester by combining ab initio calculations with Langevin dipoles (LD[15]) and polarized continuum (PCM[16,17]) solvent models. It was found that for the hydrolysis of the monoanion (and dianion), the associative and dissociative reaction pathways have similar activation barriers. Recently, Hu and Brinck, by using ab initio and density functional theory methods coupled to nonspecific solvation effects, have reinvestigated the energetics of the associative and dissociative pathways for the methyl phosphate monoanion by considering the active participation of a bridging water molecule in the proton-transfer processes.[18] These authors found that dissociation of methyl phosphate monoanion into methanol and metaphosphate (eq 1) proceeds via a six-membered water-assisted transition state, **TS(6c)**, which is considerably lower in energy

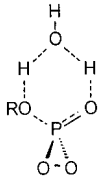

TS(6c)

(4) For reviews, see: (a) Cox, J. R., Jr.; Ramsay, O. B. *Chem. Rev.* **1964**, *64*, 317. (b) Benkovic, S. J.; Schray, K. J. In *Transition States of Biochemical Processes*; Gandour, R. D.; Schowen, R. L., Eds.; Plenum Press: New York, 1978; pp 493−528. (c) Thatcher, G. R. J.; Kluger, R. *Adv. Phys. Org. Chem*. **1989**, *25*, 99−265.
(5) Åqvist, J.; Kolmodin, K.; Florián, J.; Warshel, A. *Chem. Biol*. **1999**, *6*, R71.
(6) Florián, J.; Åqvist, J.; Warshel, A. *J. Am. Chem. Soc*. **1998**, *120*, 11524.
(7) Hart, J. C.; Hillier, I. H.; Burton, N. A.; Sheppard, D. W. *J. Am. Chem. Soc*. **1998**, *120*, 13535.
(8) Hart, J. C.; Sheppard, D. W.; Hillier, I. H.; Burton, N. A. *Chem. Commun*. **1999**, 79.
(9) Kirby, A. J.; Varvoglis, A. G. *J. Am. Chem. Soc.* **1967**, *89*, 415.
(10) This special mechanism was proposed by Kirby and Varvoglis[9] in the late 1960s to account for the reaction rate difference observed between monoanions and dianions (e.g., at 100 °C the dianion of methyl phosphate is cleaved by P−O bond-breaking 800-fold less rapidly than the monoanion[11]) and the fact that the hydrolysis rate of phosphate monoester monoanions is much greater than that of the corresponding diesters at the same pH. It is supported by a very small entropy of activation and the value of $\beta_{lg} = -0.27$, reflecting the proton transfer to the leaving group in the rate-determining transition state. The latter value led the authors to consider that complete or partial proton transfer must have occurred in the rate-limiting transition state. Kirby and Varvoglis then concluded that the hydrolyses of the monoanions of esters with leaving groups more basic than phenol (i.e., all alkyl esters) occur with rapid pre-equilibrium formation of the zwitterion $RO^+(H)PO_3^{2-}$, followed by P−O bond fission in the rate-limiting step k_z (Scheme 1, top). In contrast, when leaving group basicity drops below that of phenol, the authors came to the conclusion that proton transfer becomes partially rate-determining and occurs simultaneously with leaving group departure (Scheme 1, bottom). This picture is supported by the observation of a negative deviation of the Brönsted linear plot, log k_{hyd} vs pK_{ROH}, for leaving groups less basic than phenol (for which $\beta_{lg} = -0.16$), and by the fact that the solvent isotope effect values, k_{H_2O}/k_{D_2O}, reverse on going from esters with poor leaving groups ($k_{H_2O}/k_{D_2O} = 0.87$ for methyl phosphate[12]) to esters with very good leaving groups ($k_{H_2O}/k_{D_2O} = 1.45$ for 2,4-dinitrophenyl phosphate[9]).
(11) Wolfenden, R.; Ridgway, C.; Young, G. *J. Am. Chem. Soc.* **1998**, *120*, 833.
(12) Bunton, C. A.; Llewellyn, D. R.; Oldham, K. G.; Vernon, C. A. *J. Chem. Soc.* **1958**, 3574.
(13) Florián, J.; Warshel, A. *J. Am. Chem. Soc.* **1997**, *119*, 5473.
(14) Florián, J.; Warshel, A. *J. Phys. Chem. B* **1998**, *102*, 719.
(15) Florián, J.; Warshel, A. *J. Phys. Chem. B* **1997**, *101*, 5583.

than the four-centered transition state that is required in the absence of a water molecule (Scheme 1, bottom). They concluded that the dissociative pathway—via the rate-limiting water-assisted transition state **TS(6c)**—is favored over the associative one by more than 10 kcal/mol of free energy in solution.[19] The computed activation energy reported for the dissociative mechanism (29.0 kcal/mol) is in excellent agreement with the experimental estimate based on the measured rate constant at 373 K (30.7 kcal/mol[12]).

More recently, Admiraal and Herschlag, by using reactivity comparisons from available experimental data, also concluded that the associative mechanism, in the form of the substrate-assisted general base catalysis (eqs 3 and 4), is an unlikely alternative to the classical dissociative mechanism.[20] However, the arguments put forward in this study were severely criticized by Glennon et al.,[21] who retorted that there is no point in ref 20 that can be used as a valid argument to exclude the substrate-assisted general base mechanism of eqs 3 and 4.

The free energy profile calculated by the groups of Warshel[14] and Brinck[18] for the dissociative hydrolysis of methyl phosphate monoanion (eq 1) involves two transition states (surrounding metaphosphate intermediate) in which proton transfer contributes significantly to the reaction coordinate. Thus, according to these theoretical studies, a substantial, *normal* (>1) kinetic isotope effect is expected whether the proton transfer occurs directly or through intervening water molecules (for example, the calculated value of $k_{H_2O}/k_{D_2O} = 2.3$ was reported for the concerted proton transfer via the four-centered transition state shown in Scheme 1; see ref 14). However, the small, slightly *inverse* (<1) kinetic isotope effect value of 0.87 measured for methyl phosphate monoanion[12] rather suggests that in alkyl esters the proton transfer occurs in a fast pre-equilibrium step and not in the rate-limiting step. Thus, perhaps one of the most important features of the dissociative alternative is the assumption that alkyl monoanions undergo hydrolysis by a special *stepwise* mechanism involving anionic zwitterions $RO^+(H)PO_3^{2-}$ as kinetically relevant intermediates.[22]

Overall, despite the extensive information, some points of discussion concerning the dissociative pathway of phosphate monoester monoanions still need to be clarified: (1) Are anionic zwitterions $RO^+(H)PO_3^{2-}$ stable intermediates (minima) along the reaction coordinate in aqueous solution (Scheme 1)? If anionic zwitterions were to intervene as local minima in the reaction, then other important questions spring to mind: (2) Are these species kinetically relevant intermediates? (3) How are they specifically solvated by water molecules, and (4) what is the exact number of H_2O molecules playing a key role in their stability/reactivity? (5) Does phosphoryl transfer from $RO^+(H)PO_3^{2-}$ to H_2O proceed through a metaphosphate intermediate by an elimination−addition mechanism, referred to as $D_N + A_N$ in the IUPAC nomenclature[23] (Scheme 2, stepwise),

Scheme 2. Schematic View of Possible Mechanistic Pathways for the Hydrolysis Reaction of Phosphate Monoester Monoanions Involving Anionic Zwitterion Intermediates[a]

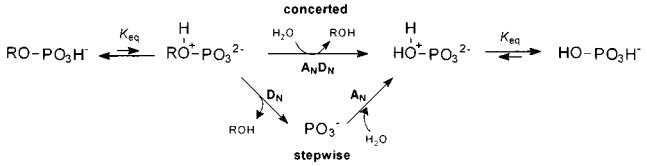

[a] Anionic zwitterions may react along a stepwise dissociative pathway involving unimolecular elimination of free, uncoordinated metaphosphate ion ($D_N + A_N$ mechanism), or along a concerted phosphoryl-transfer pathway in which the water nucleophile enters and the alcohol leaving group departs in a single step, with no intermediate (A_ND_N mechanism). Note that the first step of the stepwise process corresponds to the k_z step of Scheme 1.

or does it proceed directly to the zwitterionic form of orthophosphate ion by an in-line nucleophilic displacement at phosphorus (A_ND_N mechanism) with no discrete PO_3- intermediate (Scheme 2, concerted)?

In this and our related paper,[1] an attempt is made to provide some answers to these questions. This paper is concerned with the mechanism of the dissociative hydrolysis reaction of methyl phosphate monoanion; the other paper[1] provides a theoretical description of anionic zwitterions $RO^+(H)PO_3^{2-}$ and explores, according to the supermolecule approach, the specific role played by H_2O molecules on the prototropic rearrangement K_{eq} (Scheme 2).

In this report, we have reinvestigated the free energy profiles for the dissociative pathway of $CH_3OPO_3H^-$ (**1**) and $CH_3OPO_3H^-\cdot H_2O$ (**1a**) by performing geometry searches both in the gas phase and with the polarized continuum solvent model PCM. We provide theoretical evidence that the dissociative phosphoryl transfer occurs from the hydrated tautomeric form $CH_3O^+(H)PO_3^{2-}$ in the rate-determining step.

Methods

All calculations were performed with the Gaussian 98 set of programs[24] using hybrid density functional methods (B3LYP) which have been shown to perform well in earlier studies involving charged phosphates.[18,25] A double-ζ plus polarization valence basis set[26] was employed for each atom including hydrogen. For oxygen atoms, s and p diffuse functions were added ($\zeta_s = 0.108151$ and $\zeta_p = 0.070214$). Standard pseudopotentials developed in Toulouse[26] were used to describe the atomic cores of all non-hydrogen atoms. Molecular geometries of stationary points (i.e., minima and transition states) involved in the hydrolysis of the methyl phosphate anion were optimized in the gas phase and/or with the standard dielectric version of the polarizable continuum model D-PCM implemented in the Gaussian 98 program (vide infra). Harmonic frequencies of the B3LYP optimized structures were calculated in order to verify that the stationary points

(16) Tomasi, J.; Persico, J. *Chem. Rev.* **1994**, *94*, 2027.
(17) Miertus, S.; Scrocco, E.; Tomasi, J. *Chem. Phys.* **1981**, *55*, 117.
(18) Hu, C. H.; Brinck, T. *J. Phys. Chem. A* **1999**, *103*, 5379.
(19) In contrast to the *dissociative* mechanism, Hu and Brinck[18] found that there is no special energetic advantage for the *associative* mechanism (eq 2) to proceed through six-membered water-assisted transition states.
(20) Admiraal, S. J.; Herschlag, D. *J. Am. Chem. Soc.* **2000**, *122*, 2145.
(21) Glennon, T. M.; Villà, J.; Warshel, A. *Biochemistry* **2000**, *39*, 9641.
(22) For highly activated phosphates, however, the situation may change in favor of the concerted proton transfer (Scheme 1, bottom). In particular, this is indicated by the much greater isotope effect in the hydrolysis of the monoanion of 2,4-dinitrophenyl phosphate ($k_{H_2O}/k_{D_2O} = 1.45$[9]). See footnote 10.
(23) Guthrie, R. D.; Jencks, W. P. *Acc. Chem. Res.* **1989**, *22*, 343.
(24) Frisch, M. J.; Trucks, G. W.; Schlegel, H. B.; Scuseria, G. E.; Robb, M. A.; Cheeseman, J. R.; Zakrzewski, V. G.; Montgomery, J. A.; Stratmann, R. E., Jr.; Burant, J. C.; Dapprich, S.; Millam, J. M.; Daniels, A. D.; Kudin, K. N.; Strain, M. C.; Farkas, O.; Tomasi, J.; Barone, V.; Cossi, M.; Cammi, R.; Mennucci, B.; Pomelli, C.; Adamo, C.; Clifford, S.; Ochterski, J.; Petersson, G. A.; Ayala, P. Y.; Cui, Q.; Morokuma, K.; Malick, D. K.; Rabuck, A. D.; Raghavachari, K.; Foresman, J. B.; Cioslowski, J.; Ortiz, J. V.; Baboul, A. G.; Stefanov, B. B.; Liu, G.; Liashenko, A.; Piskorz, P.; Komaromi, I.; Gomperts, R.; Martin, R. L.; Fox, D. J.; Keith, T.; Al-Laham, M. A.; Peng, C. Y.; Nanayakkara, A.; Gonzalez, C.; Challacombe, M.; Gill, P. M. W.; Johnson, B.; Chen, W.; Wong, M. W.; Andres, J. L.; Gonzalez, C.; Head-Gordon, M.; Replogle, E. S.; Pople, J. A. *Gaussian 98*, Revision A.7; Gaussian, Inc.: Pittsburgh, PA, 1998.
(25) Lopez, X.; Dejaegere, A.; Karplus, M. *J. Am. Chem. Soc.* **1999**, *121*, 5548.
(26) Bouteiller, Y.; Mijoule, C.; Nizam, M.; Barthelat, J.-C.; Daudey, J.-P.; Pélissier, M.; Silvi, B. *Mol. Phys.* **1988**, *65*, 295.

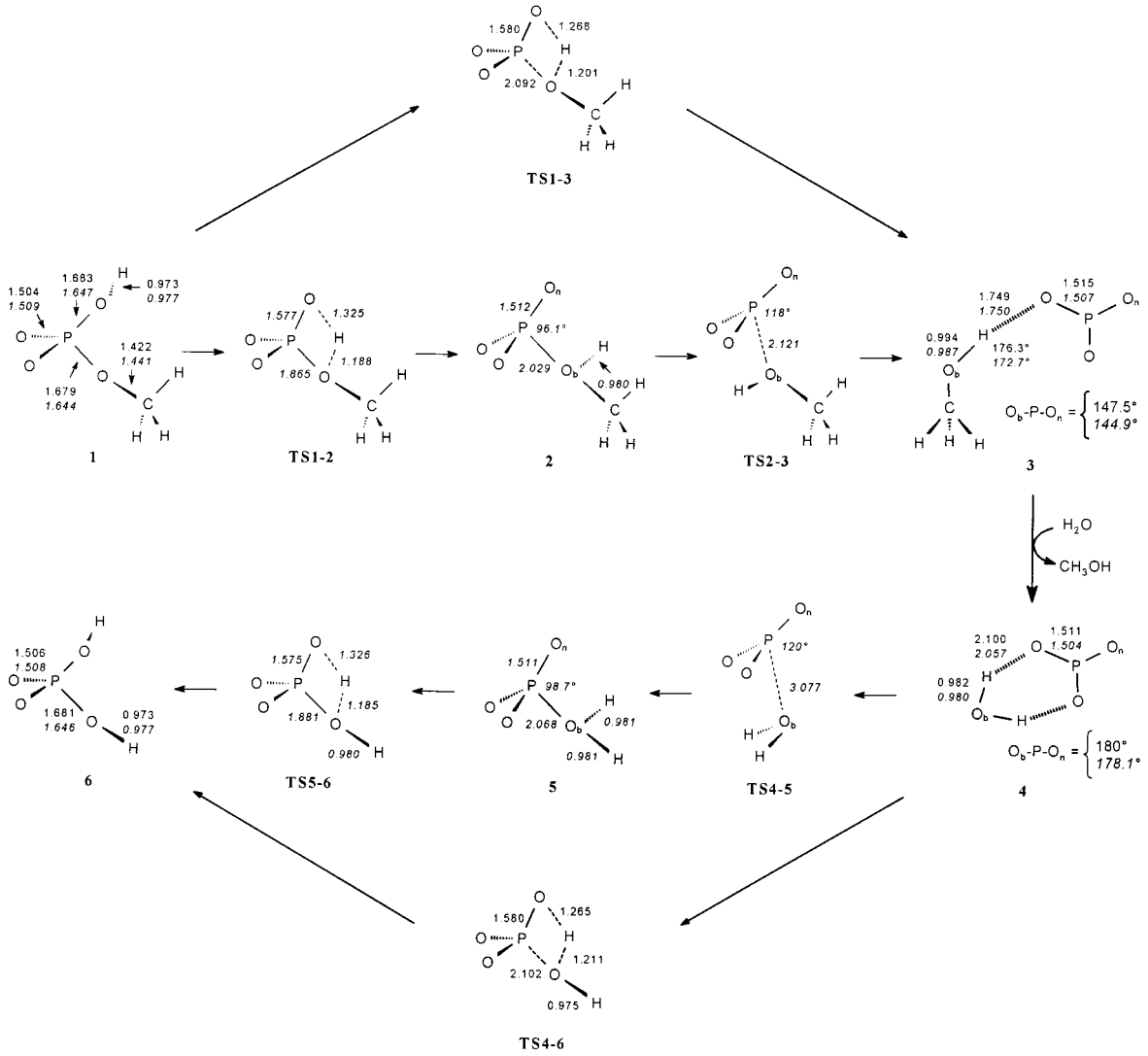

Figure 1. B3LYP optimized structures of the stationary points involved in the dissociative reaction of $CH_3OPO_3H^-$ in the gas phase (plain characters, top) and in aqueous solution (italic characters, bottom). All distances are in angstroms.

found were minima or transition states, and to obtain zero-point energies (ZPE) and thermal corrections to enthalpies and free energies at 298.15 K in the usual rigid-rotor harmonic oscillator approximation.[27]

For evaluating the effect of aqueous solvation, two approaches were used. In the first, which is of the same type as that applied by Hu and Brinck,[18] the solvation free energy (ΔG_{solv}) of a given optimized gas-phase structure and charge distribution was obtained from a single-point energy calculation at the PCM level of theory (the bulk solvent is represented by an infinite dielectric and polarizable continuum characterized by the dielectric constant of water, $\epsilon = 78.39$). In this model, the solvation free energy is composed of the work required to build a cavity in the solvent (G_{cav}) together with the electrostatic (G_{el}) and nonelectrostatic ($G_{disp} + G_{rep}$) work.[28] The sum of these terms is referred to as W_0, so that $\Delta G_{solv} = W_0$. The relative free energies in aqueous solution, referred to as ΔG_{aq}, were then calculated as the sum of the gas-phase free energies and the solvation free energies, $\Delta G_{aq} = \Delta G_{gas} + \Delta\Delta G_{solv}$, where $\Delta\Delta G_{solv}$ is the difference in solvation free energies between the stationary points considered and reactants ($\Delta\Delta G_{solv} = \Delta W_0 = \Delta G_{solv}^{SP} - \Delta G_{solv}^{R} = W_0^{SP} - W_0^{R}$). In the second approach, the relative aqueous free energies, referred to as ΔG_{PCM}, were directly obtained by calculating the vibrational modes—with the PCM[16,17] solvation correction—of the corresponding optimized PCM geometries. In this method, the quantum mechanical calculations are done in the presence of the solvation correction so that changes in geometries, charge distributions, and relative energies due to solvation can be determined. So, besides the above-mentioned W_0 term, the second approach takes into account the contributions to free energies issuing (i) from the structural differences between molecules in the gas phase and in solution (W_{geom}) and (ii) from the corresponding modifications of harmonic frequencies (W_{vib}). Modifications issuing from translation and rotation contributions (W_{trans} and W_{rot}) were neglected by assuming that the solute has a very large volume available in solvent. The free energies of solvation W_0 obtained in the first approach were then augmented in the second approach by the W_{geom} and W_{vib} terms so that $\Delta G_{solv} = W_0 + W_{geom} + W_{vib}$.

It is important to note that the treatment corresponding to the first approach implies that all the relevant stationary points of a given aqueous reaction profile must also be stationary points in the gas phase. As a result, this approach precludes the possibility that anionic zwitterions intervene as intermediates in the dissociative pathway of phosphate monoester monoanions since these species cannot be located as minima in the gas phase (see Results). Therefore, starting with the gas-phase structures of the stationary points involved in the dissociative reaction of $CH_3OPO_3H^-$ and $CH_3OPO_3H^-{\cdot}H_2O$ (Figures 1 and 2,

(27) Hehre, W. J.; Radom, L.; Schleyer, P. v. R.; Pople, J. A. *Ab Initio Molecular Orbital Theory*; Wiley-Interscience: New York, 1986.
(28) Cossi, M.; Barone, V.; Cammi, R.; Tomasi, J. *Chem. Phys. Lett.* **1996**, *255*, 327.

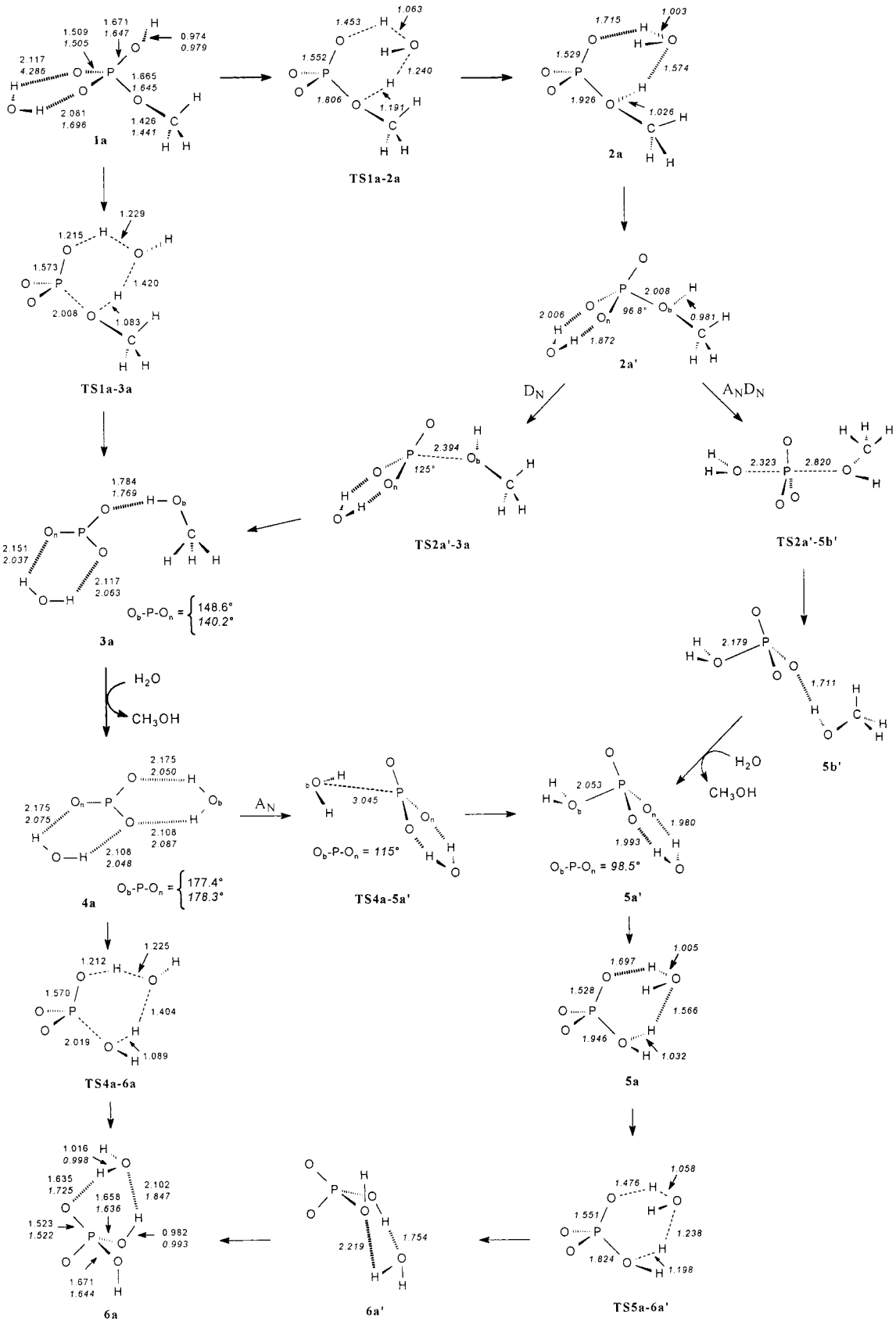

Figure 2. B3LYP optimized structures of the stationary points involved in the dissociative reaction of $CH_3OPO_3H^-\cdot H_2O$ in the gas phase (plain characters, top) and in aqueous solution (italic characters, bottom). The competing stepwise and concerted pathways in solution are indicated by $D_N + A_N$ and A_ND_N, respectively. All distances are in angstroms.

respectively) is not necessarily a good strategy to approach the actual reaction coordinate in aqueous solution. In other words, it is questionable whether the gas-phase reaction coordinate is always appropriate for exploring the free energy profile in solution, especially for those

aqueous reactions in which high-energy dipolar species are postulated as key intermediates. For this reason, we addressed the question of the possible intervention of anionic zwitterions by performing geometry searches directly with the PCM solvation model (second approach).

Calculations performed with polarizable continuum models depend on the procedure used for generating solute cavities. In continuum models, the solvent is represented by a macroscopic continuum medium (characterized by its dielectric permittivity ϵ), and the solute molecule is embedded in a cavity in this dielectric medium. To probe the molecular shape of the solute, the PCM model makes a superposition of spheres centered on atoms or atomic groups. Our calculations were done using both the conventional set of Pauling's atomic radii (the cavity is defined by interlocking atomic spheres with radii that are 1.2 times the van der Waals values; note that additional spheres may be added to make the cavity surface smoother and that these spheres may have different locations and sizes for different geometries) and the United Atom Topological Model, UATM[29] (the cavity is built automatically according to the molecular topology, hybridization, formal charge, etc.). Both procedures provide very close ΔG_{PCM} values according to the second approach (Table S3, Supporting Information) but yield ΔG_{aq} values somewhat less similar according to the first approach (Table S2, Supporting Information). Since we were unable to locate the most dissociated transition-state structures using the UATM procedure (UATM radii led to a sudden change of the total energy at critical P−O(Me) and P−O(H_2) distances), we have resorted to using the Pauling set of radii, which is completely adequate in the evaluation of relative ΔG_{PCM} values according to the second approach (Table S3).

To obtain values that are directly comparable with the experimental free energy of activation (30.7 kcal/mol at 373 K and pH 4.2) and isotope effect ($k_{H_2O}/k_{D_2O} = 0.87$ at 373 K), frequency calculations of the kinetically relevant stationary points involved in the energetically most favorable mechanisms were also performed at 373 K for both the standard and the O-deuterated molecular species $CH_3OPO_3D^-\cdot D_2O$.

Results

The gas-phase and solution structures of the reactants, transition states, reaction intermediates, and products considered in this study are depicted in Figures 1 and 2. The gas-phase thermodynamic parameters and solvation free energies of the various species relative to the reactants are given in Table 1 and in Tables S1 and S2 in the Supporting Information. The calculated thermodynamic values (relative to the reactants) of the various solution structures located with the PCM solvation model are summarized in Tables 2−4. The free energy profiles obtained in solution for the different reaction paths investigated are illustrated in Figures 3, 5, 6, and 8.

General Considerations. Full geometry optimizations with the D-PCM level of theory were successful for all the minima involved in the present study (Figures 1 and 2). This includes anionic zwitterions $RO^+(H)PO_3^{2-}$ and the corresponding molecular complexes $RO^+(H)PO_3^{2-}\cdot(H_2O)$ (R = H, Me). The transition-state structures for the proton transfer between the phosphate oxygen and the leaving or attacking group were also fully optimized with PCM. These are referred to as **TS1**−**2**, **TS5**−**6**, **TS1a**−**2a**, and **TS5a**−**6a′**. The nature of these transition states was verified by a single imaginary frequency (Tables 2 and 3) and an intrinsic reaction coordinate (IRC) calculation, leading to the expected anionic zwitterion intermediates (**2**, **5**, **2a**, **5a**) and reactants or products (**1**, **6**, **1a**, **6a′**).

Full geometry optimizations of the transition structures for the collapse of anionic zwitterions **2**, **5**, **2a**, and **5a** into the corresponding molecular complexes **3**, **4**, **3a**, and **4a**, respectively, according to an elimination−addition mechanism ($D_N + A_N$, Scheme 2) failed to converge with PCM. The shape of the reaction profiles corresponding to these "collapse" paths was then determined from a series of successful PCM optimizations performed along the presumed reaction coordinate (see Figure 4 and Figures S1−S3 in the Supporting Information). The transition structure (**TS2a′**−**5b′**) for the in-line nucleophilic substitution process (A_ND_N mechanism, Scheme 2) was similarly determined from a series of constrained optimized structures (Figure 7). In each case, the variations of the PCM energies along the selected reaction coordinate gave a curve with one maximum. The latter was used to locate the relevant transition-state structure.

For the purpose of comparing free energies of activation at 298 K, a normal-mode analysis was performed at these maxima (which is possible because the gradient of the PCM potential energy surface is essentially zero at these points). However, it is important to note that the continuum method used in the present study is clearly inadequate to identify these maxima as conventional transition states. Indeed, reactions involving large changes in charge distribution, such as the collapse of highly dipolar species, are naturally expected to exhibit profound solvent effects. In this kind of reaction, the charge distribution changes so suddenly that one can reasonably assume that the fluctuations that lead to reactive events are essentially due to solvent fluctuations, not solute fluctuations (the collapse of anionic zwitterions into molecular complexes is a barrierless process in the gas phase, vide infra). As a result, the solvent coordinate is expected to play the major role in controlling the activation barrier for the solute coordinate. For this reason, it is very unlikely that the aqueous-phase reaction coordinate would correspond to one, and only one, imaginary-frequency normal mode of the solute alone. Hence, to fully characterize and understand the nature of these barriers, a proper solvation model should include nonequilibrium solvation effects by considering both dynamical effects and the key role of solute−solvent coupling at the molecular level.[30,31]

The possible mechanisms involved in the dissociative pathway for the molecular species $CH_3OPO_3H^-$ (**1**) and $CH_3OPO_3H^-\cdot H_2O$ (**1a**) are investigated below in sections 1 and 2, respectively. For each species, there is a step that involves exchanging the methanol formed in the reaction for an additional water molecule (corresponding to transitions **3** → **4** for $CH_3OPO_3H^-$ (Figure 1) and **3a** → **4a** or **5b′** → **5a′** for $CH_3OPO_3H^-\cdot H_2O$ (Figure 2)).

1. Dissociative Reaction of $CH_3OPO_3H^-$. The simplest possible reaction that can be used to model the dissociation of methyl phosphate monoanion into PO_3^- and methanol is an intramolecular proton-transfer process proceeding via a four-membered transition state. The structures of the stationary points involved in this mechanism are presented in Figure 1 with selected geometrical parameters. In the gas phase, the proton transfer between the phosphate oxygen and the methoxy oxygen of **1** occurs via a four-membered transition state (**TS1**−**3**) which was shown, by frequency and IRC calculations, to connect directly **1** to the molecular complex $PO_3^-\cdot CH_3OH$ (**3**). The

(29) Barone, V.; Cossi, M.; Tomasi, J. *J. Chem. Phys.* **1997**, *107*, 3210.

(30) For a fairly complete review on advantages and limitations of implicit solvation models, see: Cramer, C. J.; Truhlar, D. G. *Chem. Rev.* **1999**, *99*, 2161.

(31) Hwang, J.-K.; King, G.; Creighton, S.; Warshel, A. *J. Am. Chem. Soc.* **1988**, *110*, 5297.

Table 1. Relative B3LYP Gas-Phase Energy (ΔE), Zero-Point Vibrational Energy (ΔZPE), Enthalpy (ΔH), Entropy Contribution ($T\Delta S$), Gas-Phase Free Energy (ΔG_{gas}), Solvent Contribution to Free Energy (ΔW_0), Free Energy in Aqueous Solution (ΔG_{aq}), and Transition Frequencies of TSs (ν_{gas}/cm^{-1}) for the Stationary Points Involved in the Elimination−Addition Reaction of $CH_3OPO_3H^-$ in the Gas Phase at 298 K[a]

	structure[b]	Gas										
		ΔE	ΔZPE	ΔH	$T\Delta S$	ΔG_{gas}	ΔW_0[c]	ΔG_{aq}[d,e]	ν_{gas}	ΔW_{geom}[f]	ΔW_{vib}[g]	ΔG_{PCM}[h,e]
H_2O +	**1**	0.0	0.0	0.0	0.0	0.0	0.0	0.0		0.0	0.0	0.0
	TS1−3	31.3 (33.1)	−2.9(−2.8)	28.3 (30.2)	0.1 (0.0)	28.2 (30.2)	5.1 (4.2)	33.3 (34.4)	1214i	−1.7[i]	1.9[i]	33.5[i]
	3	11.2 (10.4)	−0.8 (−0.7)	10.7 (10.6)	2.5 (4.7)	8.2 (5.9)	12.7 (10.2)	20.9 (16.1)		0.0	1.4	22.3
MeOH +	**4**	9.8 (8.7)	0.4 (0.3)	10.3 (9.2)	3.2 (3.7)	7.1 (5.5)	18.2 (12.7)	22.9 (15.8)		−3.9	0.0	19.0
	TS4−6	31.9 (33.5)	−1.7 (−1.5)	29.4 (31.1)	0.4 (0.6)	29.0 (30.5)	8.2 (5.0)	34.8 (33.1)	1249i	−4.8[j]	1.0[j]	31.0[j]
	6	−0.4 (−0.1)	1.1 (1.0)	0.1 (0.3)	0.7 (0.7)	−0.6 (−0.4)	2.7 (1.2)	−0.3 (−1.6)		−3.6	−0.3	−4.2

[a] Also reported are the relative contributions (ΔW_{geom} and ΔW_{vib}) to the relative aqueous free energy (ΔG_{PCM}) directly obtained from geometry optimizations and frequency calculations performed with the PCM solvation model using Pauling radii (see text for details). Values are calculated using a double-ζ plus polarization valence basis set including diffuse functions for oxygen atoms (see Methods). All values except those for imaginary frequencies are in kcal/mol. Values in parentheses are from ref 18 (calculated at the B3LYP/6-31+G*//B3LYP/6-31+G* level of theory). [b] The numbering system for structure identification is given in Figures 1 and 2. The exchange of methanol for water (going from **3** to **4**) requires that a water molecule be infinitely separated from **1**−**3** during the first stage of the reaction and, reciprocally, that methanol be infinitely separated from **4**−**6** during the second stage. [c] Relative solvation free energy computed with the polarizable continuum model PCM by using the conventional set of Pauling radii and a dielectric constant of 78.39. Values from ref 18 (in parentheses) were obtained by using a slightly larger radius for phosphorus than that recommended by Pauling. [d] $\Delta G_{aq} = \Delta G_{gas} + \Delta W_0$. [e] For the points **4**−**6**, −2.4 kcal/mol [-RT ln(55)] has been added to the ΔG_{aq} and ΔG_{PCM} values due to the standard state difference between solutes (1 M aqueous solution) and liquid water (55 M H_2O). [f] Relative contribution to free energy issuing from the structural differences between optimized structures in the gas phase and in aqueous solution. [g] Relative contribution to free energy issuing from the variation of harmonic frequencies of optimized structures in the gas phase and in aqueous solution (the corresponding translational and rotational variations are neglected by assuming that the solute has a very large volume available in solvent). [h] $\Delta G_{PCM} = \Delta G_{gas} + \Delta W_0 + \Delta W_{geom} + \Delta W_{vib}$. [i] Value obtained from the corresponding transition state **TS1**−**2** optimized in aqueous solution, see Table 2. [j] Value obtained from the corresponding transition state **TS5**−**6** optimized in aqueous solution, see Table 2.

methanol is then exchanged for a water molecule, leading to the molecular complex $PO_3^-\cdot H_2O$ (**4**). The conversion of **4** into orthophosphate anion (**6**) proceeds via a similar pathway with a single transition state (**TS4**−**6**) that closely resembles **TS1**−**3**. Thus, under these conditions, a solvated metaphosphate intermediate is generated in a two-step $D_N + A_N$ mechanism, as shown in eq 1.

The gas-phase energies and corresponding thermochemical data of the various species relative to the reactant(s) are listed in Table 1. For the sake of comparison, the calculated values obtained by Hu and Brinck[18] at the B3LYP/6-31+G*//B3LYP/6-31+G* level of theory are also indicated in parentheses. As can be seen, both studies lead to a similar gas-phase reaction path with two transition states and a solvated metaphosphate intermediate. Table 1 also lists the relative PCM solvation free energies (ΔW_0) and free energies in solution ($\Delta G_{aq} = \Delta G_{gas} + \Delta W_0$) for the various gas-phase stationary points involved in the $D_N + A_N$ mechanism. The overall shape of the reaction profile obtained in the gas phase is unchanged upon solvation, but there is a significant change in the energetics associated with it, as shown in Figure 3. Table 1 shows that solvation effects destabilize **TS1**−**3** and **TS4**−**6** relative to the reactant(s) by 5.1 and 8.2 kcal/mol, respectively. The major effect is on the molecular complexes **3** and **4**, which are both strongly destabilized in solution by 12.7 and 18.2 kcal/mol, respectively. As a result, the relative free energies in solution (ΔG_{aq}) of **3** and **4** greatly depend on the calculated ΔW_0 values (the ΔW_0 term contributes to ca. 60% and 80% of the total free energy in solution of **3** and **4**, respectively). After consideration of solvation effects, the free energy barrier (ΔG_{aq}, **TS1**−**3**) of the elimination step (D_N) is 1.5 kcal/mol lower than the free energy barrier (ΔG_{aq}, **TS4**−**6**) of the addition step (A_N). Hu and Brinck[18] found a similar difference in free energy between the two transition states (1.3 kcal/mol) but in the opposite direction. Finally, the overall free energy change of the reaction (**1** → **6**) is almost zero (slightly negative), both in the gas phase and in solution.

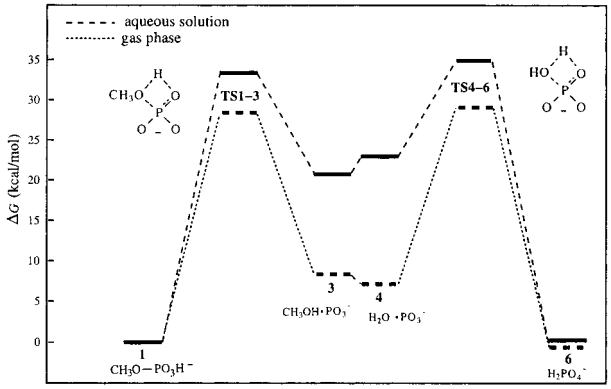

Figure 3. Free energy profile for the gas-phase dissociative reaction of $CH_3OPO_3H^-$ (dotted line, bottom) and the change in profile upon solvation (dashed line, top).

Starting with the gas-phase structures, the reactant(s), transition states, solvated metaphosphate intermediates, and products were reoptimized with the PCM solvation model to determine the changes in structure that result from solvation (Figure 1) and to calculate the associated relative free energy contributions ΔW_{geom} (Table 1). The relative contributions issuing from the variation of harmonic frequencies between optimized structures in the gas phase and in solution (ΔW_{vib} in Table 1) were also determined by calculating vibrational modes with the PCM correction. Inspection of Table 1 shows that, for the first stage of the reaction (**1** → **3**), the (relative) solvation free energy values obtained using the gas-phase structures (ΔW_0) represent a very good approximation of the overall (relative) solvation free energy $\Delta\Delta G_{solv} = \Delta W_0 + \Delta W_{geom} + \Delta W_{vib}$. The reason for this is that the free energy contributions ΔW_{geom} and ΔW_{vib} are both negligible with respect to ΔW_0. However, this is no longer true for the stationary points **4**−**6**, for which a hydrogen atom has replaced the methyl group of **1**−**3**. For these structures, PCM reoptimizations lead to significantly more pronounced solvent-stabilizing effects, as indicated by the more negative values of ΔW_{geom} (Table 1). Since the ΔW_{vib} contribution

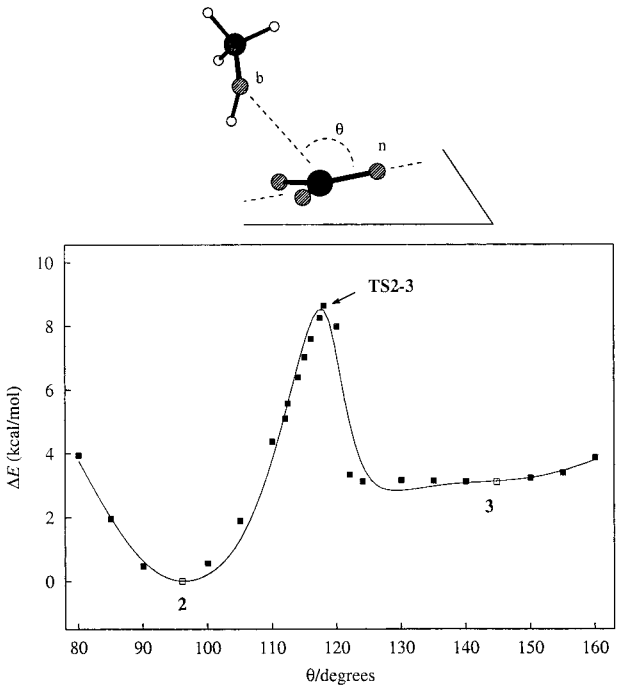

Figure 4. Relative PCM energies (ΔE), with respect to anionic zwitterion **2**, as a function of the reaction coordinate θ for the collapse of **2** into the molecular complex **3**. Solid symbols refer to optimizations performed at the fixed specified θ value while the remaining degrees of freedom were fully optimized. Positions of the fully optimized structures **2** and **3** are indicated by open symbols.

remains negligible for every stationary points of the reaction path, the overall effect of the PCM reoptimizations is to decrease the free energy barrier of the second step by 3.8 kcal/mol (compare ΔG_{aq} and ΔG_{PCM} for **TS4**−**6** in Table 1) and to slightly increase (by 0.2 kcal/mol) the free energy barrier of the first step ($\Delta G_{aq}/\Delta G_{PCM}$, **TS1**−**3**). Overall, the kinetic barrier for this reaction corresponds to the dissociation of methyl phosphate monoanion (ΔG_{PCM}, **TS1**−**3**), not to water attack on the metaphosphate ion (ΔG_{PCM}, **TS4**−**6**). Also, the reaction is found to be thermodynamically more favorable since the total change in free energy (going from **1** to **6**) is −4.2 kcal/mol in terms of ΔG_{PCM} as compared to −0.3 kcal/mol in terms of ΔG_{aq}.

While the PCM reoptimizations have a relatively small effect on the transition-state geometries (compare **TS1**−**3** and **TS1**−**2** in Figure 1), IRC calculations performed with the PCM solvation correction clearly indicate the existence of two further intermediates along the reaction path in solution. Starting from the PCM structure of each saddle point, an IRC calculation was made along the normal mode corresponding to the negative eigenvalue of the Hessian matrix. In this way, the IRC calculations enabled us to unambiguously determine what points on the potential energy surface are connected by these two maxima in solution. Thus, instead of connecting **1** and **3** (**TS1**−**3**), and **4** and **6** (**TS4**−**6**), we found that the four-membered transition structures located in aqueous solution actually connect **1** and **2**, and **5** and **6**, and were then denoted by **TS1**−**2** and **TS5**−**6**, respectively (Figure 1).

Since the reaction is expected to proceed via the zwitterionic intermediates **2** and **5**, the free energy barriers relative to them are important. Figure 4 shows how solvation leads to an activation barrier (**TS2**−**3**) for the collapse of anionic zwitterion **2** into the molecular complex **3**. We used the O_b-P-O_n bond angle formed between the bridging oxygen atom (O_b) (the oxygen of the leaving or attacking group) and one nonbridging phosphoryl oxygen (O_n) as the reaction coordinate for the collapse of anionic zwitterion **2** into the molecular complex **3** (see Figures 1 and 4 for definitions). Thus, several partial PCM optimizations were made with the constrained O_b-P-O_n angles ranging from 80° to 160° in steps of 0.5−5° (the reaction coordinate was constrained at a specified value while the remaining degrees of freedom were fully optimized). The path between hydrated metaphosphate **4** and anionic zwitterion **5** leading to the activation barrier **TS4**−**5** was obtained in a similar way (see Figure S1 in the Supporting Information). Table 2 lists the PCM energies and corresponding thermochemical data of the various solution structures relative to the reactant(s). As can be seen in Figure 5, the overall shape of the reaction profile obtained from PCM geometry optimizations is dramatically different from that obtained from solvation of the gas-phase profile (Figure 3, ΔG_{aq}). The calculated free energy barriers in solution (ΔG_{PCM}, Table 2) indicate that there are two significant local minima on the free energy profile that correspond to anionic zwitterions **2** and **5**. However, as can be seen from Table 2, the four-membered transition structures for the proton-transfer steps, **TS1**−**2** and **TS5**−**6**, are 4.6 and 9.2 kcal/mol higher in energy than the transition structures for the P−O bond-cleavage/formation steps, **TS2**−**3** and **TS4**−**5**, respectively. Thus, despite the fundamental difference between the overall shape of the free energy profiles shown in Figures 3 and 5, the predicted rate-limiting transition states for the reaction, **TS4**−**6** (ΔG_{aq}, Figure 3) and **TS1**−**2** (ΔG_{PCM}, Figure 5), are quite similar both in structure and in energy (the difference in free energy is 1.3 kcal/mol).

Table 2. Relative B3LYP−PCM Energy (ΔE), Zero-Point Vibrational Energy (ΔZPE), Enthalpy (ΔH), Entropy Contribution ($T\Delta S$), Aqueous Free Energy (ΔG_{PCM}), and Transition Frequencies of TSs (ν_{aq}) for the Stationary Points Involved in the Elimination−Addition Reaction of $CH_3OPO_3H^-$ in Aqueous Solution at 298 K[a]

	structure[b]	PCM ΔE	PCM ΔZPE	PCM ΔH	PCM $T\Delta S$	PCM ΔG_{PCM}[c]	ν_{aq}
H_2O +	**1**	0.0	0.0	0.0	0.0	0.0	
	TS1−**2**	34.6	−2.3	31.5	−2.0	33.5	1428i
	2	20.8	0.2	21.1	−0.1	21.2	
	TS2−**3**	29.3	−0.2	29.0	0.1	28.9	183i[d]
	3	23.8	−1.2	21.9	−0.4	22.3	
MeOH +	**4**	24.1	−0.1	23.8	2.4	19.0	
	TS4−**5**	26.8	−0.4	25.9	1.7	21.8	*d*
	5	20.0	1.1	20.3	0.1	17.8	
	TS5−**6**	35.3	−1.2	33.1	−0.3	31.0	1457i
	6	−1.3	1.2	−0.7	1.1	−4.2	

[a] Values are obtained from calculations (i.e., geometry optimizations and frequency calculations) performed with the PCM solvation model using Pauling radii. Units are kcal/mol for energies and cm^{-1} for imaginary frequencies. [b] Refer to footnote *b* of Table 1. [c] For **4**−**6**, −2.4 kcal/mol has been added to ΔG_{PCM} due to the standard state difference between solutes and liquid water; see footnote *e* of Table 1. [d] Note that the implicit solvation model used in the present study is inappropriate to characterize this solvent-dependent activation barrier as a conventional transition state, i.e., with only one imaginary frequency corresponding to the reaction coordinate (see text for details). Typically, vibrational analysis led to one (**TS2**−**3**) or two low (i.e., <∼200 cm^{-1}, **TS4**−**5**) imaginary frequency modes corresponding to rotations of CH_3 (**TS2**−**3**) and H_2O (**TS4**−**5**) fragments.

2. Dissociative Reaction of $CH_3OPO_3H^-\cdot H_2O$. It is well documented that current continuum models are adequate to describe reactions in solution unless some solvent molecules

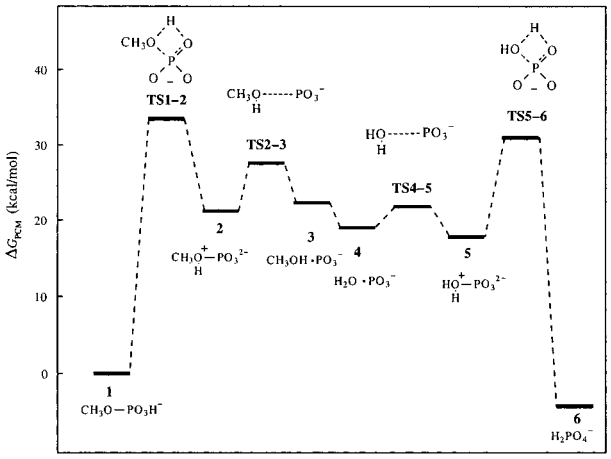

Figure 5. Free energy profile obtained from PCM geometry optimizations for the dissociative hydrolysis reaction of $CH_3OPO_3H^-$ in aqueous solution.

are directly involved in the reaction mechanism,[30] e.g., through a water-assisted proton-transfer process in which one H_2O molecule acts both as a proton acceptor and donor to facilitate the reaction. The recent theoretical study of Hu and Brinck,[18] showing that the transition structures **TS1**−**3** and **TS4**−**6** with an additional H_2O molecule are characterized by less strained six-membered rings, prompted us to locate all the stationary points involved in the reaction **1** → **6** (Figure 1) in the presence of one explicit water molecule. The optimized structures of the corresponding hydrated stationary points (**1a**, **TS1a**−**3a**, **3a**, etc.) are illustrated in Figure 2.

The gas-phase energies and corresponding thermochemical data of the stationary points involved in the lowest gas-phase activation free energy pathway for the reaction of **1a** are listed in Table S1 (Supporting Information). The key difference compared with the stationary points involved in the $CH_3PO_3H^-$ reaction is that the proton transfer between the phosphate oxygen and the leaving or attacking group proceeds via (six-membered) water-mediated transition states (**TS1a**−**3a** and **TS4a**−**6a**, Figure 2) which are 3.8 and 4.6 kcal/mol lower in free energy than the corresponding four-membered transition states **TS1**−**3** and **TS4**−**6**, respectively.[32]

In contrast to the four-membered structures **TS1**−**3** and **TS4**−**6**, the gas-phase structures **TS1a**−**3a** and **TS4a**−**6a** are markedly stabilized in solution (by 4.3 and 3.3 kcal/mol, respectively, as indicated by the negative values of ΔW_0 in Table S1). However, the molecular complexes **3a** and **4a** remain strongly destabilized (by 10.3 and 13.6 kcal/mol, respectively) so that the net result of solvation, as measured by ΔG_{aq} values, leads to an aberrant free energy profile in solution with transition states lower in energy than intermediates. Given the significant contribution of the ΔW_0 term to the free energy value ΔG_{aq}, it is possible to *apparently* resolve this aberration by using the more sophisticated UATM procedure to generate the solute cavity (see Methods). This is illustrated in Table S2 (Supporting Information), which shows how the free energy profile in solution becomes "normal" (i.e., with TSs of higher energy than intermediates) when UATM radii instead of Pauling's atomic radii are used. Note that a "normal" free energy profile in solution was also obtained by Hu and Brinck[18] by using Pauling's atomic radii for all atoms except phosphorus, for which a slightly larger radius was used (1.9 Å instead of 1.8 Å).

Our calculations indicate that geometry reoptimization in the presence of the solvent does not modify significantly the ΔG_{aq} values obtained with geometries optimized in the gas phase. As observed with the relative free energy values ΔG_{aq}, each transition state remains, in terms of ΔG_{PCM} values, 2−3 kcal/mol lower than its "corresponding" intermediate **3a** or **4a** (Table S1). The simplest explanation for this persistent aberration is that the six-membered transition structures are no longer connecting **1a** and **3a**, and **4a** and **6a**, in solution. As in the case of the $CH_3PO_3H^-$ reaction, IRC calculations clearly indicate the intervention of (hydrated) zwitterionic intermediates **2a** and **5a** (Figure 2). The latter species can then evolve according to two different pathways, as illustrated in Scheme 2.

2.1. Elimination−Addition Mechanism ($D_N + A_N$). The reaction path that corresponds to the $D_N + A_N$ mechanism depicted in Scheme 2 involves the dissociation of the cyclic complex **2a** into the corresponding metaphosphate complex **3a**. We have followed this process by first examining the effect of the displacement of the bridging water molecule in the zwitterionic complex **2a**. When the water molecule of **2a** is shifted toward the phosphate moiety, a less stable structure, denoted **2a′**, is obtained (Figure 2). The main structural difference between **2a** and **2a′** relies on the fact that, in **2a′**, the water molecule is bonded to the metaphosphate moiety (by two hydrogen bonds) without interacting with the methanol part of the structure, whereas in **2a**, the water molecule bridges the methanol and metaphosphate fragments by acting as both a hydrogen bond acceptor and donor. Although this relocation of water is likely to proceed via a barrier, the latter is expected to be smaller than the barrier for the collapse of **2a′** into the molecular complex **3a**. The transition structure corresponding to the latter barrier, **TS2a′**−**3a**, was determined from a series of constrained optimizations similar to that shown in Figure 4 (Figure S2, Supporting Information).

The path between dihydrated metaphosphate **4a** and the zwitterionic complex **5a** was obtained in a similar way, i.e., from constrained optimizations connecting **4a** and the hydrated zwitterionic form **5a′** (Figure 2), the orthophosphate analogue of **2a′**. This path is characterized by one maximum that corresponds to the transition structure **TS4a**−**5a′** (Figure S3, Supporting Information). The displacement of the water molecule from its (nonbridging) position in **5a′** toward the protonated hydroxyl ligand leads to the conformational isomer **5a**, in which water occupies a new (bridging) position that is much more effective at stabilizing the zwitterionic form of orthophosphate ion. Proton transfer then occurs through the water-assisted transition state **TS5a**−**6a′** which, according to IRC calculations, does not connect directly **5a** and **6a**, but rather **5a** and **6a′**, a local minimum of hydrated orthophosphate ion.

Table 3 lists the PCM energies and corresponding thermochemical data of the solution structures involved in the $D_N + A_N$ mechanism. The corresponding free energy profile in solution is shown in Figure 6. Table 3 and Figure 6 show that, in contrast to the $CH_3PO_3H^-$ reaction, the barriers for the proton-transfer steps (**TS1a**−**2a** and **TS5a**−**6a′**) are well below the

(32) Note that the relative energies of the four-membered transition states in the reactions of **1** and **1a** are virtually the same, suggesting that the additional water molecule must play an active role in the transition state to lower the reaction barrier effectively and thus make the reaction more feasible; see ref 18.

Table 3. Relative B3LYP−PCM Energy (ΔE), Zero-Point Vibrational Energy (ΔZPE), Enthalpy (ΔH), Entropy Contribution ($T\Delta S$), Aqueous Free Energy (ΔG_{PCM}), and Transition Frequencies of TSs (ν_{aq}) for the Stationary Points Involved in the Elimination−Addition Mechanism ($D_N + A_N$) of $CH_3OPO_3H^-\cdot H_2O$ in Aqueous Solution at 298 K[a]

	structure[b]	PCM ΔE	PCM ΔZPE	PCM ΔH	PCM $T\Delta S$	PCM ΔG_{PCM}[c]	PCM ν_{aq}
H_2O +	**1a**	0.0	0.0	0.0	0.0	0.0	
	TS1a−2a	20.3	−0.3	19.1	−2.5	21.6	795i
	2a	18.3	0.6	18.0	−2.8	20.8	
	2a′	22.6	1.8	23.7	−2.0	25.7	
	TS2a′−3a	33.5	−0.5	33.7	2.7	31.0	126i[d]
	3a	26.9	−0.9	27.0	3.4	23.6	
MeOH +	**4a**	27.5	0.0	28.0	3.4	22.2	
	TS4a−5a′	30.0	−0.6	29.2	1.7	25.1	*d*
	5a′	22.4	1.3	23.4	1.2	19.8	
	5a	17.6	2.2	18.7	−1.4	17.7	
	TS5a−6a′	19.6	1.5	19.3	−2.6	19.5	799i
	6a′	1.4	1.4	2.8	1.9	−1.5	
	6a	−1.6	1.7	−0.4	0.4	−3.2	

[a] Refer to footnote *a* of Table 2. [b] Refer to footnote *b* of Table 1 by replacing the identification numbering **1**−**6** by **1a**−**6a**. [c] For **4a**−**6a**, −2.4 kcal/mol has been added to ΔG_{PCM} due to the standard state difference between solutes and liquid water; see footnote *e* of Table 1. [d] See footnote *d* of Table 2.

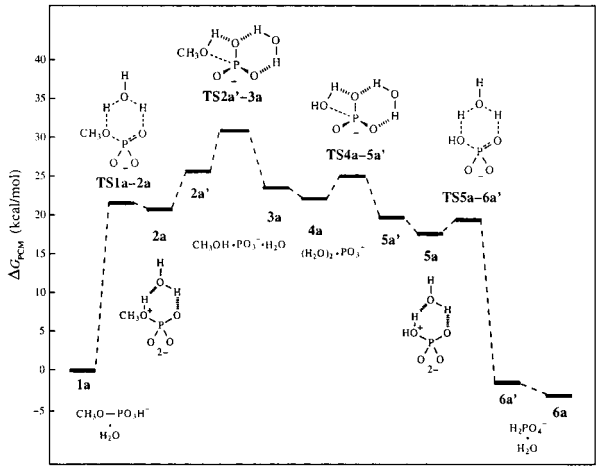

Figure 6. Free energy profile obtained from PCM geometry optimizations for the stepwise ($D_N + A_N$) hydrolysis reaction of $CH_3OPO_3H^-\cdot H_2O$ in aqueous solution.

barriers for the P−O bond-cleavage/formation steps (**TS2a′**−**3a** and **TS4a**−**5a′**). The rate-limiting step of the $D_N + A_N$ mechanism corresponds to the breakdown (via P−O bond cleavage) of the zwitterionic complex **2a′** into the metaphosphate complex **3a**. Table 3 shows that the transition structure for this process (**TS2a′**−**3a**) is 5.9 kcal/mol higher in free energy than the corresponding transition structure issuing from water attack on hydrated metaphosphate (**TS4a**−**5a′**).

2.2. Concerted S_N2(P) Mechanism (A_ND_N). The concerted A_ND_N mechanism illustrated in Scheme 2 does not involve the formation of free, uncoordinated metaphosphate ion as an intermediate. According to this mechanism, the nucleophile (nuc, H_2O) and the leaving group (lg, CH_3OH) should be weakly coordinated to phosphorus in the same rate-determining transition state.

The reaction profile for the *in-line* substitution mechanism was determined by geometry optimizations with constraints on the reaction coordinate (Figure 7). Starting from structure **2a′**,

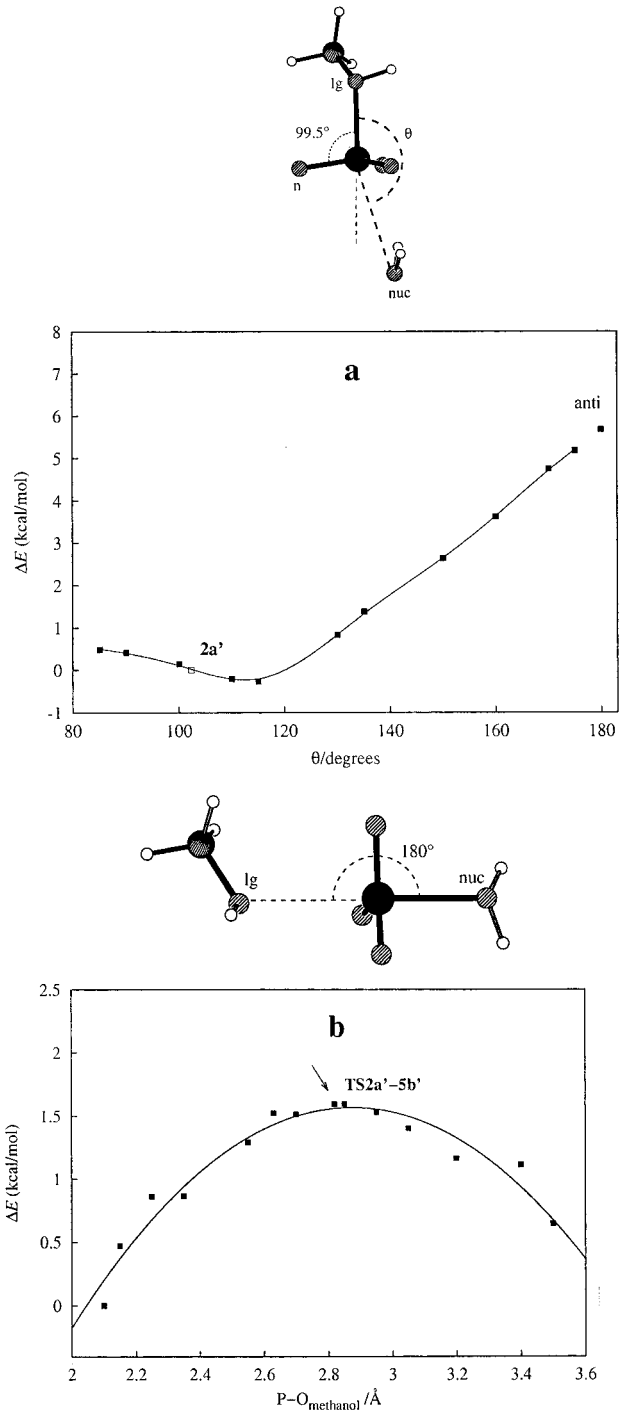

Figure 7. (a) Relative PCM energies (ΔE), with respect to the fully optimized structure **2a′** (open symbol), as a function of the reaction coordinate θ for orienting the water molecule in a position suitable for an *in-line* attack. One of the three $_{lg}O-P-O_n$ bond angles formed between the leaving oxygen (O_{lg}) and one nonbridging phosphoryl oxygen (O_n) is fixed at its optimal value calculated in **2a′** (99.5°). (b) Relative PCM energies (ΔE), with respect to the structure denoted *anti* in (a), as a function of the $P-O_{methanol}$ distance for the *in-line* ($\theta = 180°$) nucleophilic displacement (A_ND_N reaction). The first point of (b), obtained with the constraints $P-O_{methanol} = 2.1$ Å and $\theta = 180°$, is also indicated in (a) (denoted *anti*) for the purpose of continuity between the two figures.

we used the $_{lg}O-P-O_{nuc}$ bond angle θ as the reaction coordinate (see Figure 7a for definitions) to first place the water molecule in position for an in-line ($\theta = 180°$) displacement reaction. This was done by maintaining one $_{lg}O-P-O_n$ bond angle, formed

between the leaving oxygen (O_{lg}) and one nonbridging phosphoryl oxygen (O_n), at its optimal value calculated in **2a′** (i.e., 99.5°), and by gradually increasing the reaction coordinate from $\theta = 102.4°$ (the optimal value calculated in the fully optimized structure **2a′**) to $\theta = 175°$, while the remaining degrees of freedom were fully relaxed. The variation of the PCM energy along the reaction coordinate θ is depicted in Figure 7a. As can be seen, the effect of increasing θ leads to a constrained optimized structure at $\theta = 175°$ which is ca. 5 kcal/mol less stable than **2a′**. In this structure, the $P-O_{methanol}$ bond is slightly elongated (+0.062 Å) relative to its value in **2a′** (2.008 Å), and the distance between the phosphorus and the attacking oxygen, $P-O_{water}$, is slightly larger (3.4 Å) than the sum of the van der Waals radii of P and O atoms (3.3 Å). Also, hydrogen bonds between the water molecule and the nonbridging phosphoryl oxygens should be weak, with the shortest O- - -H distances in the range 2.6−2.9 Å.

The reaction coordinate for the in-line attack was then obtained as a sequence of partial PCM geometry optimizations in which the θ bond angle was constrained at 180° and the $P-O_{lg}$ distance (i.e., $P-O_{methanol}$) was gradually increased from 2.1 Å (a value close to the optimal value of 2.07 Å calculated for $\theta = 175°$, Figure 7a) to 3.5 Å, while the remaining degrees of freedom were fully optimized (Figure 7b). It should be noted that the water molecule of the first structure of Figure 7b (i.e., the point for which $P-O_{methanol} = 2.1$ Å and $\theta = 180°$) is oriented in such a way that it can hardly hydrogen bond to the nonbridging phosphoryl oxygens (O- - -H distances > 3.3 Å). In contrast to the last structure of Figure 7a ($\theta = 175°$), the first structure of Figure 7b is characterized by a calculated $P-O_{water}$ distance that is slightly smaller (3.1 Å) than the sum of the van der Waals radii of P and O atoms.

As expected, the distance to the nucleophile, $P-O_{water}$, decreases as the bond length to the leaving group, $P-O_{methanol}$, increases. The reaction profile displayed in Figure 7b shows that the transition structure (referred to as **TS2a′−5b′**) is reached at the critical $P-O_{methanol}$ distance of ca. 2.8 Å (the corresponding $P-O_{water}$ distance is 2.3 Å). In the region between the transition state and the first point of Figure 7b, the bond lengths ($P-O_{water}$) and ($P-O_{methanol}$) correlate with a slope of −1.05, reflecting the fact that, when the reaction coordinate $P-O_{methanol}$ increases, the distance to the incoming nucleophile decreases by approximately the same magnitude. In the region where the $P-O_{methanol}$ distance is greater than 2.8 Å, the correlation holds with the same trend but with a much smaller slope (−0.22), indicating that the bond to the nucleophile is well advanced ($P-O_{water} < 2.3$ Å).

Starting from the last structure of Figure 7b (i.e., the point for which $P-O_{methanol} = 3.5$ Å and $P-O_{water} = 2.12$ Å), a geometry optimization with no constraints was performed. The result led to the zwitterionic complex **5b′** (Figure 2), in which methanol is hydrogen bonded to one phosphoryl oxygen of the zwitterionic form of orthophosphate ion. The methanol of **5b′** was then exchanged for a water molecule, which gave the molecular complex **5a′** described in the preceding section. The reaction then proceeded to hydrated orthophosphate **6a** as described in the $D_N + A_N$ mechanism (vide supra).

The relative PCM energies and thermochemical data of the stationary points involved in the A_ND_N mechanism are summarized in Table 4, and the corresponding free energy profile in solution is shown in Figure 8. The *in-line* A_ND_N substitution pathway is characterized by the rate-determining transition structure **TS2a′−5b′**, in which P−O bond cleavage to the departing group and P−O bond formation to the incoming nucleophile are both involved. As observed for the $D_N + A_N$ mechanism, Table 4 shows that the barriers for the proton-transfer steps (**TS1a−2a** and **TS5a−6a′**) remain significantly lower in free energy than the barrier for the P−O bond cleavage/formation process (**TS2a′−5b′**) by 8.9 and 11 kcal/mol, respectively.

Table 4. Relative B3LYP−PCM Energy (ΔE), Zero-Point Vibrational Energy (ΔZPE), Enthalpy (ΔH), Entropy Contribution ($T\Delta S$), Aqueous Free Energy (ΔG_{PCM}), and Transition Frequencies of TSs (ν_{aq}) for the Stationary Points Involved in the Concerted $S_N2(P)$ Mechanism (A_ND_N) of $CH_3OPO_3H^-\cdot H_2O$ in Aqueous Solution at 298 K[a]

	structure[b]	PCM ΔE	PCM ΔZPE	PCM ΔH	PCM $T\Delta S$	PCM ΔG_{PCM}[c]	ν_{aq}
H_2O +	**1a**	0.0	0.0	0.0	0.0	0.0	
	TS1a−2a	20.3	−0.3	19.1	−2.5	21.6	795i
	2a	18.3	0.6	18.0	−2.8	20.8	
	2a′	22.6	1.8	23.7	−2.0	25.7	
	TS2a′−5b′	29.4	−0.2	28.4	−2.1	30.5	190i[d]
	5b′	22.4	−0.5	21.8	0.2	21.6	
MeOH +	**5a′**	22.4	1.3	23.4	1.2	19.8	
	5a	17.6	2.2	18.7	−1.4	17.7	
	TS5a−6a′	19.6	1.5	19.3	−2.6	19.5	799i
	6a′	1.4	1.4	2.8	1.9	−1.5	
	6a	−1.6	1.7	−0.4	0.4	−3.2	

[a] Refer to footnote *a* of Table 2. Values for **1a−2a′** and **5a′−6a** are reported from Table 3. [b] The numbering system for structure identification is in Figure 2. The exchange of methanol for water (going from **5b′** to **5a′**) requires that a water molecule be infinitely separated from **1a−5b′** during the first stage of the reaction and, reciprocally, that methanol be infinitely separated from **5a′−6a** during the second stage. [c] For **5a′−6a**, −2.4 kcal/mol has been added to ΔG_{PCM} due to the standard state difference between solutes and liquid water; see footnote *e* of Table 1. [d] This frequency, which corresponds to the selected reaction coordinate, was obtained along with two additional lower imaginary frequencies corresponding to rotational modes of CH_3 and H_2O fragments.

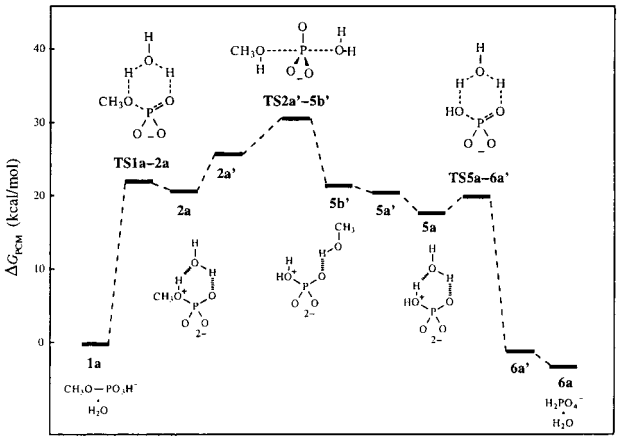

Figure 8. Free energy profile obtained from PCM geometry optimizations for the concerted (A_ND_N) hydrolysis reaction of $CH_3OPO_3H^-\cdot H_2O$ in aqueous solution.

Discussion

Nonspecific Solvation Effects: Dissociative Reaction of $CH_3OPO_3H^-$. The key result of our PCM geometry optimizations is that the phosphoryl proton of methyl phosphate can transfer to the methoxy group without involving P−O bond

cleavage between the esterified oxygen and phosphorus. Thus, the bulk solvent effect, represented by a polarizable continuum model, confirms the long-standing proposal that the zwitterionic species **2** intervenes as an intermediate in the dissociative hydrolysis of **1** (Figure 1).[9] This result contrasts sharply with our gas-phase results which, as previously reported by the groups of Brinck[18] and Warshel[14], clearly indicate that the reaction proceeds from the four-centered transition state **TS1**−**3** directly to the metaphosphate intermediate and methanol (the ion−molecule complex **3** in Figure 1). It is clear that solvating the gas-phase reaction path (by calculating hydration free energies of the gas-phase stationary points) will not change the qualitative nature of the reaction coordinate in solution. There is, however, an important change because of the change in the energetics, as shown in Figure 3. Otherwise, the reaction coordinate in solution will remain dominated by simultaneous proton transfer coupled with P−O bond cleavage, and no change in mechanism will be detected between the two phases. In contrast, the effect of aqueous solvation via the complete optimization of all geometrical variables at the PCM level allows the prediction of a mechanistic change involving anionic zwitterions **2** and **5** as reaction intermediates.

The concerted character of reactions **1** → **3** and **4** → **6** in the gas phase (Figure 1) appears to be enforced by the nonexistence of the dipolar species **2** and **5** in the absence of additional stabilization effects provided by the bulk solvent. The zwitterionic species **2** (respectively **5**), which would be the expected intermediate in a stepwise mechanism for nucleophilic addition of a methanol (respectively water) molecule to metaphosphate ion, is predicted by quantum mechanical calculations to be unbound in the gas phase.[33] Our DFT calculations indicate that as methanol and metaphosphate ion approach along the minimum-energy path of the gas-phase potential energy surface, their interaction is wholly repulsive for all separations, i.e., P- - -$O_{methanol}$ distances, less than ca. 2.7 Å.[34] Consequently, uncatalyzed formation of methyl phosphate anion **1** (from MeOH + PO_3^-) is forced to proceed by a concerted proton-transfer mechanism involving a four-centered transition state, as shown in Scheme 1. According to the principle of microscopic reversibility, dissociation of **1** (the reverse reaction) will proceed via the same transition structure (**TS1**−**3** in Figure 1) directly into the molecular complex **3**. Inclusion of dielectric effects in the calculations ($\epsilon = 78.39$) is sufficient to stabilize the zwitterionic species **2** and **5** so that the reaction paths **1** → **3** and **4** → **6** of Figure 1 are no longer forced to proceed via a concerted mechanism in solution.

The selected geometrical parameters for the four-membered transition structures involved in Figure 1 indicate that the bulk solvent effect alters the gas-phase positions of these TSs along the reaction coordinate. Comparison of the gas-phase and solution structures, **TS1**−**3** and **TS1**−**2**, clearly indicates that the proton transfer to the leaving group is more advanced in solution than it is in the gas phase, while the opposite is observed for the associated P−O bond-breaking process. Insofar as the dissociative character of these species is usually judged from a decrease in P−O bonding (between phosphorus and the esterified oxygen) on going from the reactant to the transition state, one may conclude that the gas-phase structure **TS1**−**3**, with a P−$O_{methanol}$ bond distance of 2.092 Å, is more dissociated than its solution counterpart **TS1**−**2**, for which P−$O_{methanol}$ = 1.865 Å. Similarly, P−O distances indicate that the solution structure **TS5**−**6** represents an earlier transition structure along the reaction path **6** → **4** than the corresponding gas-phase structure **TS4**−**6**.

Moreover, examination of the imaginary frequencies given in Tables 1 and 2 suggests that, despite obvious structural similarities, **TS1**−**3** and **TS1**−**2** are intrinsically different transition states. Indeed, granted that molecular complexes and transition states are generally much more floppy in solution than in the gas phase,[14] one would expect the greatest imaginary frequencies for the gas-phase structures, thus confirming that transition states become significantly looser in aqueous solution. Instead, the imaginary frequencies of the solution structures **TS1**−**2** and **TS5**−**6** are 214 and 208 cm^{-1} greater than those of the corresponding gas-phase structures **TS1**−**3** and **TS4**−**6**, respectively (Tables 1 and 2). This result is quite unusual as it reflects, in a sense, the "floppier" nature of the gas-phase structures relative to the solution structures. The simplest way to rationalize this observation is to consider that the gas-phase and solution transition states are intrinsically different, in other words, that they do not connect the same reaction intermediates in their respective phase.

As shown in Figure 4, solvation leads to an activation barrier for the collapse of anionic zwitterion **2** into the molecular complex **3**. The appearance of this barrier in solution originates from the less favorable (+ 7.6 kcal/mol) free energy of solvation of **3** relative to **TS1**−**3** (−60.8 vs −68.4 kcal/mol), and from the fact that there is an intermediate structure along the reaction coordinate between **TS1**−**3** and **3**, structurally close to **TS1**−**3**, for which solvation stabilization is maximum. This particular structure corresponds to the anionic zwitterion **2**, for which W_0 = −79.9 kcal/mol. Consequently, the fact that solvent stabilization sharply *increases* on going from **TS1**−**3** to the zwitterionic structure **2** (gain of 11.5 kcal/mol in stabilization), and then strongly *decreases* on going from **2** to the molecular complex **3** (loss of 19.1 kcal/mol in stabilization), makes structure **2** a significant local minimum on the potential energy surface in aqueous solution. Indeed, the calculated free energy barriers toward its two surrounding transition states **TS1**−**2** and **TS2**−**3** are 12.3 and 7.7 kcal/mol, respectively (Table 2). Similarly, differential solvation introduces a barrier (**TS4**−**5**) between hydrated metaphosphate **4** and the zwitterionic form **5** of orthophosphate anion (Figure S1 in the Supporting Information). The free energy values reported in Table 2 indicate that **5** is, like anionic zwitterion **2**, a local minimum bordered by two significant barriers.

The free energy diagram for the overall reaction in solution is shown in Figure 5. Although this free energy diagram is markedly different from that depicted in Figure 3 for aqueous solution, it does not represent a so meaningful change as discussed below. Indeed, both mechanisms lead to similar predictions with regard to observable dynamical and structural properties such as hydrolysis rates, isotope effects, reaction intermediates, and stereochemical outcome.

The calculated activation barriers at 298 K for the rate-determining steps of Figures 5 and 3 (**TS1**−**2** and **TS4**−**6**) are both in reasonable agreement with the barrier derived from the measured rate of hydrolysis at 373 K (30.7 kcal/mol). However,

(33) This work and refs 14 and 18.
(34) Bianciotto, M. Ph.D. Thesis, Université Paul Sabatier, Toulouse, 2001.

as indicated in the introduction section, the experimentally determined solvent isotope effect ($k_{H_2O}/k_{D_2O} = 0.87$) does not support a rate-limiting transition state involving a proton in flight as in **TS1**−**2** or **TS4**−**6**, for which substantial positive effects are expected (i.e., $k_{H_2O}/k_{D_2O} > 2$). Instead, this value suggests that the proton transfers are fast and uncoupled with the rate-limiting P−O bond-breaking or -forming process. In other words, since proton transfer does contribute significantly to the reaction coordinate in the potentially rate-limiting transition structures of Figures 3 (**TS1**−**3**/**TS4**−**6**) and 5 (**TS1**−**2**/**TS5**−**6**), one can reasonably conclude that the corresponding mechanisms are probably not valid in solution.

Furthermore, both mechanisms lead to the formation of the solvated metaphosphate ion as an intermediate (structures **3** and **4** in Figure 1). The question of whether this anion is actually formed as a discrete intermediate during phosphoryl transfer in aqueous solution remains uncertain. There appears to be no evidence that requires its formation for solvolysis reactions in aqueous solution.[35] Any reaction of a chiral phosphate ester that would proceed along a reaction pathway involving symmetrically solvated metaphosphate ion, as *implicitly* suggested in the reaction paths of Figures 3 and 5, must produce a racemic product. However, this stereochemical prediction contrasts strongly with experimental observation. Knowles et al. found that the stereochemical outcome for aqueous alcoholosis of phenyl phosphate monoanion and 2,4-dinitrophenyl phosphate dianion (made chiral by the use of oxygen isotopes) is a complete inversion of configuration at phosphorus.[36] These stereochemical results were interpreted as evidence against the intermediacy of a diffusible, symmetrically solvated, metaphosphate ion in protic media having nucleophilic and solvating properties close to the water phase.[37]

In conclusion, it is confirmed that anionic zwitterions **2** and **5** intervene as reaction intermediates in the hydrolysis of the methyl phosphate anion. However, nonspecific solvation effects indicate that these species, although located on the potential energy surface with significant potential well depths, are not kinetically relevant intermediates. By and large, confrontation with accumulated experimental aspects of this reaction indicates that the use of an implicit solvation model alone leads to unsatisfactory results. This suggests the need for a discrete/continuum model including both specific and bulk contributions.

Specific and Bulk Solvent Effects: Dissociative Reaction of $CH_3OPO_3H^-\cdot H_2O$. In accord with the recent theoretical study of Hu and Brinck,[18] we found that bifunctional participation of one water molecule is of crucial importance in assisting proton transfer to the leaving (or attacked) group. Our gas-phase calculations indicate that the energy barriers associated with the concerted transformations **1** → **3** and **4** → **6** of Figure 1 are dramatically reduced when the latter reactions occur via the six-centered transition structures **TS1a**−**3a** and **TS4a**−**6a** of Figure 2. However, inclusion of just one specifically solvating water molecule is clearly insufficient to stabilize the $RO(H)^+PO_3^{2-}$ species in the gas phase.[40] Consequently, as observed for **1**, the dissociative reaction of **1a** in the gas phase proceeds directly to the solvated metaphosphate intermediate **3a**. Similarly, the hydrated orthophosphate product **6a** is directly obtained from **4a** via the transition structure **TS4a**−**6a** as depicted in Figure 2.

PCM geometry optimizations show that there is not a significant structural change in the $RO(H)^+PO_3^{2-}$ unit due to the presence of one surrounding H_2O molecule, as indicated by the geometrical parameters provided in Figures 1 and 2 (compare the naked species **2** and **5** of Figure 1 with the corresponding hydrated species **2a**/**2a′** and **5a**/**5a′** of Figure 2). Also, in a bridging position such as that adopted in structures **2a** and **5a**, the additional water molecule has only a very small effect on the free energy values of **2** and **5** relative to the reactants. However, as observed in the gas phase, PCM optimizations lead to important differences between the energy barriers for the nonassisted and the water-assisted proton-transfer steps, the latter barriers being ca. 12 kcal/mol lower in free energy according to the values reported in Tables 2 and 3.

Such a reduction in the proton-transfer barriers alters significantly the free energy diagram of Figure 5. In sharp contrast with **2** and **5**, hydrated zwitterions **2a** and **5a** are, with regard to the prototropic rearrangement K_{eq} (Scheme 2), only marginally stable intermediates along the reaction coordinate. This is particularly true for **2a**, which is only 0.8 kcal/mol lower in free energy than **TS1a**−**2a**.[41] By contrast, the barriers for the P−O bond cleavage and formation processes are slightly increased upon the introduction of a complexing water molecule. Thus, the overall effect of specific solvation on the $D_N + A_N$ mechanism of Figure 5 is a dramatic change in the nature of the rate-limiting transition state of the reaction pathway. As can be seen in Figure 6, the kinetic barrier for the $D_N + A_N$ reaction of **1a** corresponds to the P−O bond cleavage of the (hydrated) tautomeric form $CH_3O^+(H)PO_3^{2-}$. Thus, because the full proton-transfer step **1a** → **2a** precedes the rate-limiting P−O bond cleavage step, one can expect a low (i.e., close to unity) kinetic isotope effect for this mechanism.

The calculated activation barrier for the rate-determining step of the $D_N + A_N$ mechanism of Figure 6 is 30.3 kcal/mol at 100 °C, in very good agreement with the experimental value of 30.7 kcal/mol. The corresponding barrier calculated at the same temperature for the O-deuterated molecular species $CH_3OPO_3D^-\cdot D_2O$ is 30.2 kcal/mol. This leads to the calculated solvent isotope effect value of 0.87,[42] that is, exactly the same as the experimentally determined value at 100 °C.

The free energy diagrams obtained for the $D_N + A_N$ reaction pathway (Figures 5 and 6) have important implications with regard to conclusions that can be reached about the aqueous solution chemistry of metaphosphate ion. Our calculations suggest that phosphoryl-transfer reactions cannot proceed in aqueous solution through a diffusionally equilibrated metaphosphate intermediate. The calculated free energy barrier at 25 °C

(35) Herschlag, D.; Jencks, W. P. *J. Am. Chem. Soc.* **1989**, *111*, 7579 and references therein.
(36) Buchwald, S. L.; Friedman, J. M.; Knowles, J. R. *J. Am. Chem. Soc.* **1984**, *106*, 4911.
(37) Note, however, that in similar stereochemical experiments performed in nonhydroxylic solvents[38] or in the sterically hindered protic solvent *tert*-butyl alcohol,[39] varying amounts of racemic products were observed, consistent with the involvement of metaphosphate as a diffusionally equilibrated intermediate.
(38) Friedman, J. M.; Knowles, J. R. *J. Am. Chem. Soc.* **1985**, *107*, 6126.
(39) Freeman, S.; Friedman, J. M.; Knowles, J. R. *J. Am. Chem. Soc.* **1987**, *109*, 3166.
(40) Despite an intensive search on the potential energy surface, the monohydrated zwitterionic intermediates **2a**, **2a′**, **5a**, and **5a′** of Figure 2 could not be located without including dielectric effects in the calculations.
(41) This result reveals the elusiveness of anionic zwitterions in solution. Indeed, even the simple observation of these species appears to be unlikely due to the presence of just one specifically solvating water molecule.
(42) Based on the conventional transition state theory: $k_{H_2O}/k_{D_2O} = \exp[(\Delta G_D^{\pm} - \Delta G_H^{\pm})/RT]$.

for the uncatalyzed addition of one H_2O molecule to PO_3^- (**4** → **TS4**−**5**), or to its hydrated form $PO_3^-{\cdot}H_2O$ (**4a** → **TS4a-5a′**), is 2.8−2.9 kcal/mol. This barrier is lower than the free energy barrier for diffusion apart of an encounter pair in water solution (estimated to be ca. 3.2 kcal/mol on the basis of the rate constant value $k_d = 10^{10}$ s^{-1} for diffusional separation of two species in an encounter complex). Consequently, our calculations predict that if a metaphosphate intermediate is formed during phosphoryl transfer, it should not have a lifetime sufficient to allow diffusion; it should be captured by water before it can escape the solvation sphere. It is important to note that a similar conclusion was reached by Lightcap and Frey from accumulated experimental evidence concerning the hydrolysis of monothiopyrophosphate (MTP) in aqueous solution.[43]

The corresponding free energy barriers for capturing metaphosphate (**3** → **TS2**−**3**) and hydrated metaphosphate (**3a** → **TS2a′**−**3a**) with a methanol molecule are 6.6 and 7.4 kcal/mol, respectively. The fact that water is much more efficient than methanol in capturing metaphosphate reveals that metaphosphate reacts as a selective electrophilic species.[44] However, since methanol is so much more powerful a nucleophile than water, one must conclude that the discrimination between these two nucleophiles is entirely controlled by solvation effects, not by nucleophilicity. Consequently, the absence of selective phosphorylation observed in mixed alcohol−water solvents, such as in various methanol−water mixtures,[9,45] cannot be explained in terms of an unselective reaction of metaphosphate with hydroxylic solvents, as has been widely speculated.[46] The slight selectivity observed in some cases has been interpreted in terms of selective solvation,[9] the product distribution reflecting the solvent distribution in the first solvation shell of metaphosphate.[47] Again, this analysis is based on the view that metaphosphate is a highly reactive and unselective electrophilic species. In contrast, our calculations show (i) that there is a clear discrimination between methanol and water and (ii) that this discrimination originates from a significant differential solvation effect between anionic zwitterions **2** and **5**. The important point here is that the *solvent-induced selectivity* of metaphosphate manifests in the opposite direction of what is expected from nucleophilicity. Therefore, product distributions explained by recourse to the partitioning of discrete metaphosphate between hydroxylic solvents should be interpreted with great caution.

Finally, it is important to note that the hydrolysis of MTP,[43] and probably that of alkyl phosphomonoester monoanions as well,[48] differs from the hydrolysis of many other phosphate monoesters most fundamentally in that the kinetics for their cleavage reveals the absence of nucleophilic participation in the transition state. This is consistent with the view that these compounds undergo hydrolysis through a true dissociative mechanism and a discrete metaphosphate intermediate. It should be noted also that the $D_N + A_N$ mechanism of Figure 6 is not in conflict with the stereochemical results observed with phosphate monoesters (vide supra).[36] Indeed, our calculations suggest that metaphosphate should be trapped by ambient water molecules *before* the leaving methanol has diffused away. Therefore, collapse to an acceptor H_2O molecule is not expected to be equally probable from each face of the planar species. This should lead to an inversion of configuration at phosphorus, as observed with aryl phosphates.

The dissociative $D_N + A_N$ reaction pathway of Figure 6 is consistent with *all* the experimental data so far reported on the hydrolysis reaction of the methyl phosphate anion. However, this mechanism could well be associated with or bypassed by an alternative S_N2 mechanism involving a transition state with both nucleophile and leaving group loosely coordinated to a metaphosphate-like species. Because most of the recent literature on phosphomonoester hydrolysis has given more support to this alternative, we have explored this possibility by calculating the barrier height associated with an in-line nucleophilic displacement at phosphorus.[49]

In the concerted A_ND_N reaction pathway of Figure 2, the transfer of the phosphoryl group from anionic zwitterion **2** to the H_2O molecule occurs only when the latter is properly positioned to receive the metaphosphate fragment, as illustrated in Figure 7. The transition state for phosphoryl transfer (**TS2a′**−**5b′**, Figure 2) is characterized (i) by a high degree of bond cleavage between the leaving methanol and the phosphoryl group in flight, (ii) by the presence of the acceptor nucleophile H_2O, and (iii) by the existence of weak bonding between the phosphoryl group and H_2O. Thus, the dissociative A_ND_N reaction of **1a** does not involve metaphosphate ion as an intermediate, although the central part of **TS2a′**−**5b′** has metaphosphate character. The stereochemical consequence of such a mechanism on chiral methyl [^{16}O,^{17}O,^{18}O]phosphate monoanion would be a complete inversion of configuration at phosphorus and, therefore, would agree with the stereochemical findings discussed above for aryl phosphates.[50]

The free energy diagram for the A_ND_N reaction pathway (Figure 8) shows that the phosphoryl-transfer step is rate-

(43) Lightcap, E. S.; Frey, P. A. *J. Am. Chem. Soc.* **1992**, *114*, 9750. To our knowledge, this study constitutes the only positive evidence that supports the occurrence of a discrete PO_3^- intermediate in aqueous solution. However, it was concluded that PO_3^- is not diffusionally equilibrated with solvent. Metaphosphate is so reactive with nucleophiles that it cannot escape from its solvation sphere; it is captured by water or another nucleophile that competes with water in solvating MTP.

(44) The differences in the barrier heights observed between methanol and water for capturing PO_3^- ($\Delta\Delta G = 6.6 - 2.8 = 3.8$ kcal/mol) and $PO_3^-{\cdot}H_2O$ ($\Delta\Delta G = 7.4 - 2.9 = 4.5$ kcal/mol) correspond to selectivity values (as measured by the rate constant ratio k_{H_2O}/k_{MeOH}) of ca. 600 and 2000, respectively.

(45) Chanley, J. D.; Feageson, E. *J. Am. Chem. Soc.* **1963**, *85*, 1181.

(46) Metaphosphate is expected to react with the two solvent species in a purely statistical manner such that the product distribution reflects the bulk solvent distribution.

(47) It is possible that the solvation shell of metaphosphate is different in composition from the bulk solvent due to specific attractive or repulsive forces between the reactant and a specific solvent component. Even though metaphosphate is an unselective species, this preferential solvation should lead to a discrepancy between the product distribution and the bulk solvent distribution.

(48) Although the hydrolysis of the monoanion of 2,4-dinitrophenyl phosphate is strongly catalyzed by substituted pyridines, no reaction is detectable with 2-nitrophenyl, 4-nitrophenyl, and phenyl phosphate monoanions, indicating that the nucleophilic catalysis becomes rapidly less significant as the pK_a of the leaving group increases. On the basis of this trend, it is expected that the monoanions of alkyl esters are insensitive to nucleophilic catalysis (the kinetic data for alkyl monoanions are lacking because of the incompatibility of reactive phosphate monoanions, at pH ≈ 4, with the free base forms of the more reactive, and therefore more basic, amine nucleophiles). See: Kirby, A. J.; Varvoglis, A. G. *J. Chem. Soc. B* **1968**, 135.

(49) Preliminary calculations indicate that a non-in-line concerted A_ND_N mechanism involves a high-energy path and thus does not provide a reasonable reaction pathway for phosphoryl transfer.

(50) The question as to whether the stereochemical results obtained for aryl phosphates[36] can apply to alkyl phosphates remains problematic. However, the monoanion of phenyl phosphate involved in these stereochemical studies behaves as a typical phosphate monoester in that its rate of hydrolysis is maximal at pH 4 and greater than that for its dianionic form. In addition, as discussed in footnote 10, the possibility that this compound hydrolyzes as the methyl phosphate ester through the stepwise pathway shown in Scheme 1 cannot be excluded.

determining (**TS2a′**−**5b′**). Calculations performed at 100 °C indicate that this mechanism has an activation barrier that is only 0.7 kcal/mol higher than that calculated for the $D_N + A_N$ reaction of Figure 6. Since the calculated value for k_{H_2O}/k_{D_2O} at 100 °C is 1.07, one must conclude that the A_ND_N mechanism is also in very good agreement with the kinetic data reported for the hydrolysis of **1**. However, the fact that the $D_N + A_N$ and A_ND_N mechanistic alternatives have very similar activation barriers is indicative that the putative kinetic advantage of nucleophilic participation of one H_2O molecule in the transition state is insignificant. This result appears to contradict the widely accepted assumption, often made without discrimination between mono- and dianions, that the A_ND_N mechanism should provide the lowest energy pathway for the hydrolysis reaction of typical phosphate monoesters in aqueous solution.

Conclusions

Gas-phase and aqueous solution DFT calculations have been performed on the molecular species $CH_3OPO_3H^-$ (**1**) and $CH_3OPO_3H^-\cdot H_2O$ (**1a**) to complement earlier theoretical work on the dissociative hydrolysis reaction of methyl phosphate monoanion. Bulk effects were taken into account with the polarizable continuum model PCM either by solvating the gas-phase reaction paths or by performing geometry searches directly in the presence of the solvation correction. Our results can be summarized as follows:

(1) In the gas phase, the dissociative reaction of **1** and **1a** is a stepwise elimination−addition process ($D_N + A_N$) involving metaphosphate ion as an intermediate. The elimination (respectively, addition) step proceeds through a cyclic transition state in which proton transfer to the leaving (respectively attacked) group occurs synchronously with P−O bond cleavage (respectively formation). By acting as a proton-transfer relay in six-centered transition structures, the water molecule of **1a** lowers the free energy barriers of both steps.

(2) Solvation of the gas-phase reaction profiles of **1** and **1a** gives rise to important changes in the energetics which may lead to *abnormal* free energy profiles in solution, depending on the procedure used for generating solute cavities. Otherwise, no change in mechanism is observed between the two phases. The substantial (>2) solvent isotope effect predicted by the solvated $D_N + A_N$ reaction paths of **1** and **1a** contrasts strongly with the experimentally determined value ($k_{H_2O}/k_{D_2O} = 0.87$).

(3) The effect of aqueous solvation via PCM geometry optimizations establishes the existence of anionic zwitterions $RO^+(H)PO_3^{2-}$ (R = Me, H) as reaction intermediates. Thus, *complete* proton transfer to the leaving group can occur in aqueous solution without triggering the breaking of the P−O bond. It is concluded that the gas-phase reaction coordinate cannot reliably describe the condensed-phase reaction coordinate.

(4) For the reactant species **1**, it is found that the barrier for the prototropic rearrangement $CH_3OPO_3H^- \rightarrow CH_3O(H)^+PO_3^{2-}$ is rate-determining, while for **1a**, the kinetic barrier corresponds to the collapse of the hydrated zwitterion into solvated metaphosphate: $CH_3O^+(H)PO_3^{2-}\cdot H_2O \rightarrow CH_3OH\cdot PO_3^-\cdot H_2O$.

(5) The $D_N + A_N$ reaction of **1a** is energetically favored over the $D_N + A_N$ reaction of **1** and, more importantly, is in excellent agreement with experimental data: the calculated activation barrier at 100 °C is very close to the experimentally determined value (30.3 vs 30.7 kcal/mol), and the calculated solvent isotope effect (k_{H_2O}/k_{D_2O}) of 0.87 matches exactly the measured value for methyl phosphate monoanion.

(6) Metaphosphate monoanion produced in the $D_N + A_N$ reaction of **1a** is captured by a *single* water molecule before it can escape its solvation sphere. This result suggests that metaphosphate is probably not a liberated intermediate in aqueous solution. Also, in contrast to the view held for 40 years, our calculations reveal that PO_3^- may react as a selective electrophilic species with ROH nucleophiles. However, the observed selectivity of metaphosphate manifests in the opposite direction of what is expected from nucleophilicity, water being much more effective than methanol in capturing PO_3^-. This *solvent-induced selectivity* arises from a better solvation of the addition product $H_2O^+PO_3^{2-}$ as compared to $CH_3O^+(H)PO_3^{2-}$.

(7) The present results do not allow a distinction to be made between the stepwise $D_N + A_N$ path discussed above and a concerted A_ND_N path proceeding via a dissociative (metaphosphate-like) transition state (both mechanisms were found to have very similar activation barriers and solvent isotope effects). Note that, although a concerted *associative* mechanism can be in principle considered a limiting case of the A_ND_N mechanism, the energetics of such a mechanism was not elucidated in this study. Work is in progress in our laboratory to address this important issue. Concerning the dissociative mechanism, in the absence of any direct experimental evidence of nucleophilic catalysis, it seems reasonable to conclude that metaphosphate ion can occur as a discrete species in this reaction. There is also the possibility that a water molecule quenches the forming metaphosphate by acting as a nucleophile in the transition state—but certainly there is no evidence that *requires* it.

Acknowledgment. This work is dedicated to Prof. J. Périé on the occasion of his retirement. We thank the Centre Informatique National de l'Enseignement Supérieur (CINES), Montpellier, France, for a generous allocation of computer time (project pqt1073).

Supporting Information Available: Tables S1−3 and Figures S1−3, see text (PDF). This material is available free of charge via the Internet at http://pubs.acs.org.

JA0200948